Columbia University
in the City of New York

LAMONT GEOLOGICAL OBSERVATORY
PALISADES, NEW YORK

Technical Report on Seismology No. 26

Crustal Structure and Surface Wave Dispersion Part IV, the Atlantic and Pacific Ocean Basins

LAMONT GEOLOGICAL OBSERVATORY

(Columbia University)

Palisades, New York

* * *

Technical Report No. 26

CU 32-53-AF 19(122)441 GEOL.

Crustal Structure and Surface Wave Dispersion,

Part IV, the Atlantic and Pacific Ocean Basins

by

Jack Oliver, Maurice Ewing and Frank Press

The research reported in this document has been made possible through support and sponsorship extended by the Geophysics Research Division of the Air Force Cambridge Research Center under Contract AF 19(122)441. It is published for technical information only and does not represent recommendations or conclusions of the sponsoring agency.

January 1953

Abstract

Properties of the ocean-ocean floor acoustical system pertinent to the study of microseisms are deduced from earthquake surface waves. First mode Love and Rayleigh waves on seismograms from the Honolulu station indicate that no submerged land masses of continental proportions underlie the Pacific Ocean as outlined by the earthquake belt. Similar results are obtained for parts of the North Atlantic. The method, however, is insensitive to relatively small or thin structures. The Easter Island Rise is anomalous and possibly includes a thin layer of continental-like material.

Some earthquakes cause a short period train of surface waves to be propagated over oceanic paths. The beginning of the train is identified as Love wave motion. The later part of the train, which is not definitely identified, is very similar in character to long period microseisms. These waves are sharply attenuated at continental margins but propagate easily through either continents alone or oceans alone. The sources show distinct geographical preferences.

INTRODUCTION

Studies of elastic wave propagation in the acoustical system consisting of the oceans and underlying rock strata fall into three general classifications: (1) seismic refraction and reflection using explosive sources, (2) the body and surface waves of earthquakes, (3) microseisms. Of the three, the study of microseisms is the most difficult because less is known about the source and about the path over which the waves travel. A considerable gain can be made, then, by studying the other methods in order to fix certain parameters that might remain in doubt if the field of study were restricted to microseisms alone. These parameters include the elastic constants of the media and their geometrical configuration as well as a basic understanding of the geologic features. This paper deals with earthquake surface waves which are particularly pertinent since microseisms appear to be a similar phenomenon.

Although surface waves are the most conspicuous feature on most seismograms, their study has not received great emphasis, so that at present there are many unexplained or partially understood surface wave arrivals. As late as 1950, Ewing and Press[10]* presented a theory which for the first time was able to explain the entire train

*Superscripts refer to the list of references at the end of the paper.

of ordinary crustal Rayleigh waves, providing the path was predominantly oceanic, i.e. no continental or shallow water segments of appreciable length lay on the arc of the great circle between the epicenter and the recording station. The theory was experimentally confirmed in that report and in subsequent papers[11,1]. The theory of Love waves has been well-known for considerably longer and several investigators, e.g. Gutenburg[15], Wilson[28], Evernden[9] and Byerly[3], have deduced oceanic crustal structure from Love wave dispersion.

The purpose of this study is the consideration of all types of surface waves having a preponderance of oceanic path with a view toward (a) an experimental investigation of the mechanism of propagation, (b) the reconciliation of the various crustal structures obtained from surface wave dispersion and that deduced from explosion seismology, (c) the detection of variations in crustal structure over different oceanic paths.

With these objectives in mind, a collection of records from the Honolulu installation was obtained. This station has the following advantages: (a) it is uniquely located near the center of the Pacific so that oceanic paths prevail at all azimuths, (b) its location near the center of the Pacific earthquake belt provides, over a period of a few years, sources of suitable magnitude at all azimuths, (c) the instrumentation includes matched long period horizontals with reasonably good response

at the surface wave frequencies. The chief disadvantage is the absence (with the exception of a few months in 1949-50) of a long period vertical instrument for the separation of Rayleigh and Love waves. A further familiar difficulty, inherent in the restriction to one recording station, lies in the necessity of utilizing sources that may be dissimilar, but it is felt that this is outweighed by the advantage of a single set of invariable instrumental constants. The consistency of the results is proof of the validity of this approach.

Although the Honolulu collection accounted for the majority of the data, considerable supplementary information for the Pacific Ocean was obtained from the Berkeley and Fresno stations, and from the Bermuda, Palisades, Ottawa and Kew installations for the Atlantic Ocean.

Instrumentation

The Honolulu station is operated by the U.S. Coast and Geodetic Survey. Under normal conditions two modified long-period Milne Shaw horizontals and one short period Neumann-Labarre horizontal are recording. The Milne-Shaws have a 12 second free period, gain of about 130, damping ratio of 20:1, and are oriented N-S and E-W. The Neumann-Labarre has a free period of 1.2 seconds, gain of 4800, damping ratio of 8:1, and is oriented E-W. All three drums run at a paper speed of 30mm/min. For a few months at the end of 1949 and the beginning of 1950, short and long period vertical Sprengnethers were operated, and

Those records appropriate to this study were used.

Because of the location in the midst of the Pacific Basin, background due to microseisms is particularly bad at Honolulu, especially during the winter months. This is the reason for the low gain of the long period instruments. It restricts the selection of sources to earthquakes of fairly high magnitude.

At Bermuda there are two Milne-Shaw horizontals oriented NE-SW and NW-SE, with a free period of 12 seconds, gain of 250, damping ratio about 16:1, and paper speed of 8mm/min. There is also a complete set of three component Benioffs, both long (T_o = 1, T_g = 90 secs) and short period (T_o = 1, T_g = 0.2 secs), as well as a Columbia University vertical seismograph with T_o = 12, T_g = 15 secs. The latter group of instruments has been installed during 1951 and 1952, so that the backlog of earthquake records is very scanty.

The Palisades records used in this study were taken by a matched three component set of Columbia University design with T_o = 12, T_g = 15 secs. The vertical is identical with the instrument at Bermuda. Long and short period Benioff records are also available at Palisades.

Only the Galitzin records from Berkeley were studied. These are similar in response to the Columbia instruments and have T_o = 12, T_g = 12 secs. for all three components. Fresno has a three component set of Sprengnethers.

Ottawa has two Milne-Shaw horizontals and a Benioff vertical,

both long and short period. Kew has a three component set of Galitzins with the free period of the seismometer and of the galvanometer equal. The periods of the Kew instruments all fall in the range of 12-23 seconds.

Experimental Procedure

Selection of Records: Tables 1, 2 and 3 list all the earthquakes used in this study. Fig. 1 shows their geographic distribution. For the most part the Pacific earthquakes are limited to the years 1947-48-49-50. Those making first mode of Rayleigh waves at Honolulu are plotted as squares. They were chosen for selected azimuths and paths, and general clarity, and do not represent all the earthquakes making this type of surface wave during the four year period. The triangles designate earthquakes that made a surface wave of higher frequency. These represent all the earthquakes of this type in the Pacific belt during the four year period, providing they were of sufficient magnitude to be located and to be recorded at Honolulu. The reason for the more thorough search for this type is their rather peculiar geographical distribution to be discussed later.

To take advantage of the superior instrumentation several records of Hawaiian earthquakes recorded at Berkeley and Fresno were added to the Pacific collection.

The Atlantic earthquakes were restricted to 1950-51-52 because of the recent additional instrumentation at Bermuda and because the Palisades station has only been in operation during that period.

Identification of Wave Trains: The absence of a long period vertical at the Honolulu station for use in distinguishing Love and Rayleigh waves is undoubtedly the greatest difficulty in the entire study. To overcome this, the first records to be studied were chosen from quakes at azimuths very near to due north, south, east or west. With this orientation, Love waves appear only, or in practice much more strongly, on the transverse instrument and Rayleigh waves on the longitudinal, e. g., see Fig. 5A, where the earthquake is nearly due west of Honolulu. G and R indicate the beginning of the Love and Rayleigh wave train respectively. After some experience and confidence had been achieved sight identification was virtually certain at the intermediate azimuths. The advantages of this procedure were described by Neumann[19]. It is fortunate that, in general, the long period Love wave train, or "G" wave, has died away before the beginning of the Rayleigh waves. For the intermediate azimuths, of course, it is always possible to check the particle motion in the horizontal plane by combining the results of the two components.

Method of Reading Dispersion: The method of reading and plotting the dispersed train of waves was previously discussed in Ewing and Press[12] and Pekeris[21] The procedure is to assign consecutive numbers to each peak, or trough, or zero, beginning with the first and continuing until the train becomes ragged. Each number is then plotted against the arrival time of the corresponding point. The slope of the resulting curve at any point is a measure of the frequency at the time

corresponding to the point. The group velocity is then calculated and plotted against the period. After the train becomes ragged, periods are obtained by averaging over groups of 5 or 6 peaks that appear relatively undisturbed. The time is measured to the center of the group.

Continental Correction - For the portion of the path of known continental character (the 1000 fathom curve was used as the boundary here as in previous papers) a correction was made using the continental Rayleigh velocity curve of Brilliant and Ewing[1] or Wilson and Baykal[29]. These continental curves have some uncertainty and may vary somewhat from place to place, but in all cases studied here the differences between the curves are insignificant because the percentage of continental path is small.

Epicentral Location - The preliminary epicentral determinations of the U. S. Coast and Geodetic Survey, occasionally supplemented by the preliminary locations of the Jesuit Seismological Association were used throughout the investigation. The differences between these epicentral locations were nearly always small enough to be negligible in the present study. No earthquakes deeper than 100 km were studied.

Theory

Elastic theory provides, in general, for two types of waves at a free surface, now commonly called Love and Rayleigh waves after their discoverers. Love or SH waves are shear waves polarized hori-

zontally. They depend for their existence on horizontal layering of some sort, and are always dispersive, i. e. different periods travel with different phase and group velocities. Rayleigh waves, on the other hand, can exist at the free surface of a homogeneous semi-infinite solid in which case they are non-dispersive, but in the actual case of the layered earth, they too are dispersive. This is evident intuitively because the shorter wave lengths are confined largely to the upper layer and derive their velocity from its elastic properties, whereas the longer wavelengths penetrate deeper and are more affected by the properties of the deeper layer. We will consider each type separately in the following discussion. These symbols will be used:

α = compressional wave velocity in a solid

β = shear " "

V = compressional wave velocity in water

σ = Poisson's ratio

H = layer thickness

λ = wavelength

$k = \frac{2\pi}{\lambda}$ = wave number

f = frequency

$\gamma = \frac{Hf}{V} = \frac{H}{\lambda}$ = non dimensional term to frequency

C = phase velocity

U = group velocity

ρ = density

Subscripts 1, 2, 3 refer to layers numbered from top to bottom. n refers to number of mode.

Rayleigh Waves: Several investigators have examined the problem of elastic wave propagation in a water layer overlying a semi-infinite solid layer. A bibliography and a brief review of their results is found in Press et al[22]. Their results, in general, are not suited to earthquakes with predominant ocean path. The Ewing-Press theory considers a liquid layer having the elastic properties and density of sea water overlying an elastic solid with properties appropriate to the material below the Mohorovicic discontinuity. In this simplified structure the sediments are lumped with the water as the liquid layer, and the bottom material is considered an average for any layering present in the bottom. They used the following equation, first given by Stoneley[27], which is a relation between phase velocity and wave length:

$$\tan\left(K_m H\sqrt{\frac{c_m^2}{V^2}-1}\right)=\frac{\rho_2}{\rho_1}\frac{\beta_2^4}{c_m^4}\frac{\sqrt{\frac{c_m^2}{V^2}-1}}{\sqrt{1-\frac{c_m^2}{\alpha_2^2}}}\left[4\sqrt{1-\frac{c_m^2}{\alpha_2^2}}\sqrt{1-\frac{c_m^2}{\beta_2^2}}-\left(2-\frac{c_m^2}{\beta_2^2}\right)^2\right]$$

The group velocity is obtained by graphical or numerical differentiation from $U = C + kH\frac{\partial C}{\partial (kH)}$. These curves are shown in Fig. 2 in dimensionless form. The values assigned to the constants are tabulated in Table 4. The equation is trancendental and the method of solution is to choose a C and then solve for KH. Since the tangent function is oscillatory there will be an infinite number

of solutions. The order of each solution or mode is designated by the subscript n. In practice only the lower orders are encountered and only the first two are shown on the graph.

The depth of the source is an important factor in deciding how much energy is put into each mode, and Press et al[22] showed that only the first mode is appreciable for source depths greater than twice the water depth under a flat bottom.

Fig. 6 shows only the portion of the curve applicable to the present surface wave study. Group velocity is plotted against period and the depth of water is taken as a parameter.

As would be expected on physical reasoning, the shorter wavelengths are most sensitive to the depth of the liquid so that the steep portion of the curve on the left is most useful in determining this quantity experimentally. In fact, the curve is so steep that it is possible to get a quick estimate of the depth simply by measuring the period anywhere along the late, long drawn out coda.

The long wavelengths, virtually unaffected by the water depth, are quite sensitive to the shear velocity of the basement rocks. A variation of this quantity would raise or lower the flat portion of the curve, which is asymptotic to the Rayleigh wave velocity (=. 92B for $\sigma = 1/4$) in the lower medium.

An intermediate layer or layers, not considered in the original theory, would have its greatest influence on the wavelengths lying between

the two extremes. To determine the magnitude of the effect of such a layer, Jardetzky and Press[18] solved the three layer problem of a liquid layer overlying two solids for the two cases listed in Table 4. Case II is intended to represent as closely as possible the results of refraction shooting in the North Atlantic Basin. Case I differs in that the velocity of the intermediate layer is what might be expected from a granitic material. Their results showed that for the range of periods involved it is impossible to distinguish Case III from the simpler two layer case of Ewing and Press[10]. Case I could be differentiated from the others only if the thickness of the intermediate layer were at least as great as the depth of water. So in order for a layer of continental type granitic rock to be detected under the Pacific Basin by Rayleigh wave dispersion it would need to be at least 5-1/2 km average thickness over the entire path.

The period equation for the three layer case of Jardetsky and Press is:

$$\ell_0 + \ell_1' \sinh(\eta_1 KH)\sinh(\eta_3 KH) + \ell_2' \sinh(\eta_1 KH)\cosh(\eta_3 KH) + \ell_3' \cosh(\eta_1 KH)\sinh(\eta_3 KH) + \ell_4' \cosh(\eta_1 KH)\cosh(\eta_3 KH) + \left[\ell_1'' \sinh(\eta_1 KH)\sinh(\eta_3 KH) + \ell_2'' \sinh(\eta_1 KH)\cosh(\eta_3 KH) + \ell_3'' \cosh(\eta_1 KH)\sinh(\eta_3 KH) + \ell_4'' \cosh(\eta_1 KH)\cosh(\eta_3 KH)\right] \left[\tanh(\eta_0 KH)\right] = 0$$

where

$$\ell_0 = 4\left(2 - V_0^2\frac{V^2}{\beta_2^2}\right)G_1$$

$$\ell_1' = \left(2 - V_0^2\frac{V^2}{\beta_2^2}\right)^2\frac{1}{\eta_1\eta_3}G_2 - 4\eta_1\eta_3 G_3$$

$$\ell_2' = -\left(2 - V_0^2\frac{V^2}{\beta_2^2}\right)^2\frac{\rho_3}{\rho_2}\frac{\eta_2}{\eta_1}V_0^4\frac{V^4}{\beta_2^4} + 4\frac{\rho_3}{\rho_2}\eta_1\eta_4 V_0^4\frac{V^4}{\beta_2^2}$$

$$\ell_3' = -\left(2 - V_0^2\frac{V^2}{\beta_2^2}\right)^2\frac{\rho_3}{\rho_2}\frac{\eta_4}{\eta_3}V_0^4\frac{V^4}{\beta_2^4} + 4\frac{\rho_3}{\rho_2}\eta_2\eta_3 V_0^4\frac{V^4}{\beta_2^4}$$

$$\ell_4' = \left(2 - V_0^2\frac{V^2}{\beta_2^2}\right)^2 G_3 - 4G_2$$

$$\ell_1'' = -\frac{\rho_1\rho_3}{\rho_2^2}\frac{\eta_1\eta_4}{\eta_0\eta_3}V_0^8\frac{V^8}{\beta_2^8}$$

$$\ell_2'' = \frac{\rho_1}{\rho_2}\frac{\eta_2}{\eta_0}V_0^4\frac{V^4}{\beta_2^4}G_3$$

$$\ell_3'' = \frac{\rho_1}{\rho_2}\frac{1}{\eta_0\eta_3}V_0^4\frac{V^4}{\beta_2^4}G_2$$

$$\ell_4'' = -\frac{\rho_1\rho_3}{\rho_2^2}\frac{\eta_2}{\eta_0}V_0^8\frac{V^8}{\beta_2^8}$$

and

$$G_1 = XZ - \eta_2 \eta_4 W Y$$

$$G_2 = Z^2 - \eta_2 \eta_4 Y^2$$

$$G_3 = \eta_2 \eta_4 W^2 - X^2$$

$$X = \frac{\rho_3}{\rho_2} V_0^2 \frac{V^2}{\beta_2^2} - 2\left(\frac{\mu_3}{\mu_2} - 1\right)$$

$$Y = V_0^2 \frac{V^2}{\beta_2^2} + 2\left(\frac{\mu_3}{\mu_2} - 1\right)$$

$$Z = \frac{\rho_3}{\rho_2} V_0^2 \frac{V^2}{\beta_2^2} - V_0^2 \frac{V^2}{\beta_2^2} - 2\left(\frac{\mu_3}{\mu_2} - 1\right)$$

$$W = 2\left(\frac{\mu_3}{\mu_2} - 1\right)$$

$$\eta_0 = \sqrt{1 - V_0^2}$$

$$\eta_1 = \sqrt{1 - V_0^2 \frac{V^2}{\alpha_2^2}}$$

$$\eta_2 = \sqrt{1 - V_0^2 \frac{V^2}{\alpha_3^2}}$$

$$\eta_3 = \sqrt{1 - V_0^2 \frac{V^2}{\beta_2^2}}$$

$$\eta_4 = \sqrt{1 - V_0^2 \frac{V^2}{\beta_3^2}}$$

The thicknesses of the two layers are taken to be equal.

For this paper the second mode of this equation was calculated using the constants of Case III. The curves are shown in Figs. 2 and 3, and the computed values in Table 5. The only appreciable deviation from the two layer case falls in the period range 5-1/2 to 8 seconds for H = 5.57 km. The magnitude of the difference is of the order of the experimental error so that if a second mode train were definitely identified, it is improbable that the dispersion would give much useful information about the intermediate layering unless the variations in dimensions or elastic constants were greater than those chosen for the calculations.

For the simple two layer case, particle motion at the surface of the solid was shown to be retrograde elliptical for both the first and second modes.[22] For the three layer case the calculations were not carried out because of the prohibitive amount of time and labor required. However, it seems probable, at least for the long waves, that the particle motion of the first mode must also be retrograde elliptical at the surface of the upper solid. It also seems probable that this is the case for the second mode as well. Sezawa's M_2 wave[26], which the authors would term second mode for the case of a solid layer over a semi-infinite solid, was shown to have progressive elliptical motion. However, the branch of the equation corresponding closest to M_2 for the three layer case falls at a shorter period than the two branches studied here, i. e. out of the recorded surface wave periods.

Love Waves - The theory of Love wave propagation is well known[2]. The period equation for the two media case is

$$\mu_1 \left(1-\frac{c^2}{\beta_1^2}\right)^{1/2} - \mu_2 \left(\frac{c^2}{\beta_2^2}-1\right)^{1/2} \tan kH_1 \left(\frac{c^2}{\beta_2^2}-1\right) = 0$$

Fig. 4 shows the curves for Case III. The second mode was computed for Case III but the values of the periods are so small that they fall well below the range covered in this investigation. The chief features of the curve to be noted are that (a) the long waves are asymptotic to the shear velocity in the lower medium and (b) the duration of the train is determined largely by the contrast of the two shear velocities. The effect of a change in layer thickness is to rearrange in a simple manner the distribution of periods in this time interval.

Choice of Constants - The question of the values of the elastic constants chosen for the calculations is an important one, since the accuracy of the values determines the degree of usefulness of the method in exploration of the crust. The constants that were chosen for the calculations have the following basis. Case II, the simple two layer case was the first Rayleigh wave dispersion curve to be calculated because the equations and computations are the simplest. The value of 7.9 km/sec for the compressional wave velocity was chosen as representative of the early seismic refraction results in the Atlantic ocean basin. Improvements in the refraction techniques enabling longer profiles to be carried out resolved the original single basement layer

into two layers of compressional velocities 6.9 and 8.1 km/sec respectively. These numbers were used in the three layer computation, Case III, of Jardetzky and Press. More recent refraction results[20] in the Atlantic have centered about a mean of 6.5 and 7.9, although the values run from 6.26±.17 to 6.63±.17 and 7.56±.18 to 8.27±.27 km/sec. In the Pacific, Raitt[24] has given values of 6.75 and 8.1 for typical deep water profiles between Hawaii and the west coast of North America. The value of 5.5 km/sec was taken as typical of continental rock.

As the surface wave calculations for the three layer case are long and tedious it is not practical to compute separate curves for the different values. However, the effect of small changes in the constants can be estimated fairly well. From the two three layer cases in which the velocity of the intermediate layer was 5.5 and then 6.9 km/sec, resulting in curves differing by an amount barely discernible experimentally, it is evident that a change from 6.9 to 6.5 or 6.75 km/sec will, of course, fall between the first two curves and very nearly coincide with the latter. Thus the selection of an intermediate layer more in keeping with the results of recent refraction shooting will alter the theoretical curve a very slight, experimentally immeasurable amount. However, a change of the bottom layer from 8.1 to 7.9 gives a more pronounced effect. Using $\sigma = 1/4$ the shear velocities are 4.68 and 4.56 and the Rayleigh wave velocities for very long wave-

lengths 4.31 and 4.20 km/sec. The long period end of the dispersion curve is asymptotic to these latter two values so as a first approximation the curves will differ by about 0.1 km/sec for the long periods. This is about the margin of experimental error. The Love wave curve will be affected in about the same manner and degree.

The validity of the 0.25 choice for Poisson's ratio also needs to be examined. From the well known formula $1+\frac{1}{1-2\sigma}=\frac{\alpha^2}{\beta^2}$ the values in Table 6 may be obtained. The value for $\sigma=0.25$ was chosen to simplify the calculations. Earthquake data[2, 11] give a value for σ of about 0.27 for the depths and material of interest here. A first approximation to the effect of a change can be estimated by observing the change in shear velocity as above and raising or lowering the curve by that amount. This is about 0.1 km/sec for these two values of σ.

Experimental Results

First Mode Rayleigh Waves: This train of waves is of markedly sinusoidal nature and usually occupies a major portion of the seismogram (Fig. 5A). The periods range from about 35 to 15 seconds with corresponding velocities varying from 4.1 to about 1.4 km/sec. In all cases the waves fit the theory well. The theoretical dispersion curves fit the data and the particle motion, whenever determinable, is retrograde elliptical and is always in the general direction of the

plane of propagation. Thus there is no doubt that the theory has a firm basis.

There are, however, small systematic differences correlating with azimuth from Honolulu. Fig. 7 shows the thickness of the liquid layer (water + unconsolidated sediment) deduced from the low velocity part of the train. The scatter is of the order of 0.2 kilometers. Plotted on the same figure are average water depths at 15^{o} intervals of azimuth taken from H.O. charts 0526, 0527, 0528, 0529, 0823, 0824, 0825, 0826, and 5951. There is some uncertainty in these values as well because (a) the water depths are not known to sufficient precision and (b) there is some doubt as to precisely which path between epicenter and station should be followed due to lateral refraction of the surface waves. It seems reasonable that these averages might be in error by, at most, the same number, 0.2 kilometers. These uncertainties limit the precision of the experiment but it is still possible to obtain a reliable estimate of the sediment thickness from the plot.

The sediment thickness taken from Fig. 7 ranges from 0.4 km due north of Honolulu to nearly 1.2 km to the southwest. These numbers are in excellent agreement with the results of Raitt[24] using the explosion seismic refraction technique in the Pacific and with results of similar studies in the Atlantic. Furthermore, there seems to be a real trend toward thicker sediments in the southwest quadrant where island atoll groups are plen-

tiful. Also apparent from the plot are the greater basement depths in the western half of the Pacific. However, the data is scanty to the east, almost lacking in the entire N. E. quadrant due to the absence of earthquakes generating first mode Rayleigh waves, so that the accuracy of the last statement is in need of further verification.

The sediment thicknesses in the Atlantic are shown in Table 7. Water depths are from H. O. charts 0955, 0956, 0955a and 0956a. This survey is not as complete as the Pacific one because of the less convenient location of earthquakes and stations. However, the thicknesses are of the same order of magnitude, from 0.5 to 1.1 km. Only one value is over 0.6 km and in that case the path includes a sizable portion of the Mid-Atlantic Ridge where the error in the water depth may be larger.

The second phase of exploration with Rayleigh waves would involve the determination of the shear velocity in the deep rock layer from the longer wavelengths, but, in practice, the instrumental response and perhaps the frequency spectrum of energy released at the source do not allow wavelengths to be recorded that are long enough to be insensitive to the intermediate layer or layers. Thus we cannot completely isolate the deep layer shear velocity problem from the intermediate layer problem.

To study these questions the earthquakes have been grouped geographically. Fig. 8 is a plot of Rayleigh wave group velocity vs.

period for earthquakes in the Marianas. This group fits the three layer case III quite well. The path is clearly entirely oceanic. Plotted in Fig. 9 are earthquakes lying on the prolongation of the great circle path to the Marianas, i. e. the Philippine Island shocks. The points at the long period end in general lie somewhat below those for the Mariana shocks. Since it will be seen later that there is a general tendency for the long period observations to fall on or about . 1 km/sec below the theoretical curve of case III, the margin is near the limit of experimental error. It is difficult to say whether a slightly different type of layering is indicated beneath the Philippine Sea, but it may safely be concluded that layers having continental properties and dimensions are absent. These results are supported by Love wave observations given in a later section. This negates the conclusions of some geologists (see Umbgrove 27a for references) concerning the existence of the submerged Melanesian continent.

The Formosan shocks nos. 42, 42A. 42B and 46 (Fig. 10) also fall slightly below the theoretical curve. However, interpretation here is further complicated by the presence of a segment of the Ryukyu island arc over a significant portion of the great circle path to Honolulu. The correction for such a structure in such an orientation is so uncertain that any deductions concerning slight deviations from the layering assumed in Case III are not reliable. The Japanese shocks 13, 35, and 38 (Fig. 11) fall on the theoretical curve quite well

although only one shock, 35, gave waves of over 25 second period. Shocks 16 and 43 in the Kuriles (Fig. 12) gave virtually identical results with the Japanese shock although waves of over 25 second period were lacking from both. Shocks 7, 12 and 25 in the Alaskan area (Fig. 13) also fit the theoretical curve well. Shocks 7 and 25 produced waves of 30-35 second period although the former required a large continental correction. Shock 20A near Tacoma (Fig. 14) also gave an excellent fit with periods up to 30 seconds.

The next group of shocks, plotted in Fig. 15, subtends a fairly large angle from southern Mexico to central Peru. There is good agreement with the theoretical curve. The next group of earthquakes to the south includes one in Chile and two, a main shock and an aftershock, at the tip of South America (Fig. 16). Only for the latter two were waves of over 25 second period recorded. These fall below the general trend of observations by just about the minimum detectable amount. It seems probable that they have been affected by the Easter Island rise indicating a possible thickening of the intermediate layer or an additional material of slower velocity or both. This conclusion is supported by data from Love waves to be given in a later section.

The six earthquakes in the next group (Fig. 17) stretching from the Tongas to the Loyalty Islands plot very close to the theoretical curve but very slightly below it. From refraction studies near this area Raitt has found some slow velocity material (4.5-5.0 km/

sec) near volcanic islands or submerged mountains which he has tentatively identified as volcanic rock. It is possible that there might be enough of this material throughout Polynesia to account for the slightly slower surface wave velocities there. Such would also be the case for the remaining shocks, numbers 4, 18, 17 and 30 (Fig. 18) which also plot slightly low. Shocks 17 and 18, however, off New Britain certainly need allowances for the land and shallow water path. The same can be said for number 36 in the Solomons. Number 4 fits the curve well as it stands.

In summary then we can say that although slight deviations in the long period end of the Rayleigh wave dispersion curve can be detected at different azimuths from Honolulu, these deviations are small and cannot be used with certainty to deduce minor changes in crustal structure over small segments of the path. In spite of these limitations, however, the data do show conclusively that there are no major variations in the crustal structure throughout the Pacific Ocean, i. e. no submerged continental structure of significant proportions. The slightly low velocity of the long Rayleigh waves from the quakes at the tip of South America is interpreted as due to a lower velocity material in the Easter Island rise. The slightly low velocity for paths crossing the Philippine Sea would admit at most the possibility of a thin low velocity layer, but Love wave data show

no indication of its presence. The Pacific is commonly divided into two sections on petrologic evidence. These sections are separated by the "andesite line", so called because volcanic islands lying between the continents and the line frequently contain andesitic rocks, whereas those on the ocean side of the line are of olivine basalt. Although this study indicates that the areas on either side of the andesite line are similar with respect to the propagation of surface waves, it does not preclude the possibility of petrologic changes providing the dimensions of the rocks involved are thin in the sense described in the section on theory.

The majority of the plots show a tendency for the points corresponding to long wavelengths to fall below the theoretical curve. This indicates a shear velocity for the material below the Mohorovicic discontinuity about 1-3% lower than that assumed for Case III.

All the Atlantic data are plotted in Fig. 19. Scatter of the order of 0.2 km/sec is evident at the long period end of the curve, about the same order of magnitude as in the Pacific data. However, it is apparent that the same dispersion curve fits both oceans equally well so that no difference between the Atlantic and the Pacific is shown by the Rayleigh wave data.

Previous work on Rayleigh wave dispersion in the Atlantic was that of Wilson and Baykal[29] who studied the shock of 25 November

1941. Their readings from the Fordham seismogram also are plotted in Fig. 19. These readings are concordant with the new data. The readings used by Gutenberg and Richter[15] from the South Atlantic earthquakes of 28 August 1933 recorded at La Plata, and 23 February 1932 recorded at Scoresby Sound are also shown to agree in Fig. 19. The other Atlantic data of Gutenberg and Richter are not shown because large corrections for continental paths would be required.

In a recent paper Rothe[25] has concluded that the Mid-Atlantic Ridge forms the boundary between an eastern basin underlain by continental rocks and a western basin underlain by ultrabasic rocks. Although the present study gives but little coverage of the eastern basin, the data shows no evidence of a submerged continent. The available Rayleigh wave evidence favors similarity of the two basins. Coverage of the Mid-Atlantic Ridge is more complete. The Ridge produces no effect on the dispersion curves except those due to water depths.

Evernden[8] presented evidence to show that lateral refraction of Rayleigh waves could account for the deviation of the direction of approach from the azimuth of the epicenter. Qualitative observations of this study verify his conclusions and further indicate the increasing magnitude of the effect as the period of the waves decreases. An investigation of waves of much longer period (70 to 400 secs.) indicated that the effect of the continents is negligible on waves of such long wavelengths.[14]

In accordance with the findings of previous papers[11, 1], there is no evidence of the short period branch of the dispersion curve, with the exception of an occasional T phase.

First Mode Love Waves: Beginning with a long period oscillation also known as the "G" phase (Fig. 5A), this train appears only on the horizontals and particle motion is transverse. Only a very few cycles appear on the record, indicating the lack of contrast of the elastic properties of any layering of the oceanic crust. This is further confirmation of the theory that the water layer, which has no effect on Love waves, is the primary factor affecting the dispersion of Rayleigh waves. The period range of the train is from 50 seconds to about 12 seconds on the Honolulu instruments. Caution must be exercised in distinguishing "G" from SS.

Scatter in the data is large, due to the strong effect of a small segment of continental path because the dispersion is much more pronounced through the continental type rock. This is a counterpart, in reverse, of the case with Rayleigh waves where the dispersion due to the ocean path is by far the stronger. For Rayleigh waves, dispersion under continents can be studied best when some oceanic path has spread out the spectrum[1]. For Love waves the reverse is true. For example, the shock of 21 January 1952 (H 20 55 12, 4°S, 30 1/2°E) on the Tanganyika border showed a well-dispersed train at Palisades and would be suitable for measurement of Love wave dispersion across the Atlantic if records were available from a station on the west coast of Africa at the point where the coast intersects the great circle path from the epicenter to Palisades.

An additional difficulty is the discrimination against waves of long period by most seismographs and the differences between various seismographs in this connection. It is believed that, taken together, these factors can account entirely for the difference between crustal structures deduced by different investigators.

Table 1 includes a column which indicates whether or not each shock made long period Love or "G" waves at Honolulu. About two thirds did not. The better ones of the remaining third are plotted in Fig. 4. Considerable scatter is evident. The only reliable information appears to be the shear velocity in the lower layer. Neglecting the quakes from the southeast quadrant the plot shows that a shear velocity of 4.50 km/sec with the same layering as Case III fits the data well. This is slightly below the value of 4.68 km/sec used in the Rayleigh wave calculations, but is very near the shear velocity obtained under the assumption that $\sigma = .27$ in agreement with Gutenberg[17] and the compressional velocity is 8.1 km/sec as in the refraction studies. Since most of the Rayleigh wave velocities for periods greater than 20 sec fall slightly below the theoretical curve for Case III, indicating a shear velocity slightly less than 4.68 km/sec for the bottom layer, the result from Rayleigh and Love waves may be said to agree within the experimental error.

The low velocity of the long period Love waves from the southeast substantiates the deductions from the Rayleigh waves that

the Easter Island Rise is not of typically oceanic crustal structure. On the basis of PP/P amplitude ratios, Gutenberg deduced that points near and east of the Rise were of continental structure of 20-30 km thickness.[17] Although some doubt has been cast on the reliability of this method[4], it appears that the conclusions were not entirely wrong. Daly reports findings of typically continental rocks on Easter Island and suggests "that the plateau is an extensive but relatively thin slice of rock of continental type". The findings of this report tend to substantiate this, but are not conclusive evidence. From similar reasoning, the high velocity of Love waves from the Philippines is unfavorable to a thin layer of continental rocks under the Philippine Sea.

Short Period Surface Waves: A number of the records of the Honolulu collection exhibit a type of surface wave distinctly different from those previously discussed (Fig. 5, B, E). They have periods varying from about 10 or 20 seconds to 6 seconds, with corresponding velocities of 4.4 km/sec to an indeterminable lower limit of at most 2.0 km/sec. These wave have previously been noted by other investigators[5, 6, 19], but have not been studied extensively. Ewing and Press[11] and Evernden[8] pointed out the approximate fit to the second mode Rayleigh wave dispersion curve. Coulomb[6] pointed out their transverse character and suggested that they might be second mode Love waves.

In this paper the train is broken into two parts for convenience

of description. The first few cycles of the train are definitely Love waves down to a velocity of about 3.5 km/sec and period of about 7-8 seconds. The particle motion is distinctly transverse. There is little if any vertical component although evidence is meager due to the lack of a vertical instrument at Honolulu during most of the period covered by this study. The waves are absent on the Berkeley vertical record of Hawaiian shocks (Fig. 20). They are the only coherent part of the train. The dispersion fits the first mode Love wave curve calculated for Case III satisfactorily (Fig. 21). Identical trains are recorded at the Bermuda station for Atlantic and West Indian shocks. It is quite certain that this portion of the train consists of Love waves.

The second part of the train of velocity less than 3.5 km/sec is present on all three components. However, the particle motion is incoherent, i.e. no consistent orbital motion can be determined from record to record or from point to point on the same record. In view of the increasing effect of refraction at continental margins as the wavelengths become shorter as noted above, it is to be expected that these short period surface waves might become less reliable for particle motion studies. However, the transverse component shows every indication of being a continuation of the short period train (see Fig. 5, B, C). Furthermore, the amplitude of the transverse component, where distinguishable, is generally greatest. Shocks due north of Honolulu show first mode Rayleigh waves on the longitudinal instru-

ment and the short period waves on the transverse. One shock, number 71, nearly due east of Hawaii, shows almost equal amplitudes on both horizontals.

The previous observations appear to be good evidence in favor of a Love wave hypothesis for the late part of the train. However, in opposition to this point of view is the appearance of the train on the Berkeley and Bermuda verticals with an amplitude of the same order of magnitude as the horizontals. Furthermore, the dispersion roughly but not exactly fits the second mode Rayleigh wave dispersion curve (Fig. 21), the periods in general being too large for the water depth derived from first mode observations over the same path. Additionally, there is no known layer of low enough shear velocity to produce a similar dispersion in Love waves. So at present there is no concrete theoretical explanation for the later part of the short period surface wave train.

The similarity of this part of the train to long period microseisms is inescapable. The conclusions to be drawn here may be extended with certainty to microseism propagation.

Geographical Factors Relating to Presence or Absence of Various Surface Type Waves

The Honolulu collection indicated that earthquakes producing the shorter period surface waves have a peculiar geographical distribution (Fig. 1). Beginning on the Easter Island Rise they can be

traced up the west coast of North America, along the Aleutian chain and down the Kuriles to Japan. Carder[5] reports two shocks in the Marianas making this period waves at Berkeley in addition to results in agreement with the present study. A few shocks in the Solomons, Fijis and New Zealand may be added to the list as well as Hawaiian shocks recorded at Berkeley. These scattered examples make it difficult to state that the short period waves are never generated in any one area. However, it is obvious from the map that they predominate on the Easter Island Rise, the west coast of North America and the Aleutians. With the exception of the Aleutian arc, where some intermediate depth shocks are found, the seismicity of these regions

is entirely confined to shocks of shallow depth.

Shocks making both first mode Rayleigh waves and the short period surface waves were noted in the Pacific (Fig. 5, C, D). To investigate this more thoroughly, Bermuda, Palisades and Berkeley records in addition to the Honolulu ones were studied with the following results:

1. First mode Rayleigh waves are present on every shock of normal depth for which the propagation path has an adequate oceanic segment. In many cases the first mode cannot be seen on the seismogram due to masking by the stronger short period surface waves. For instance (a) on Mid-Atlantic Ridge shocks whose great circle

path to Palisades passes near to Bermuda, first mode Rayleigh waves cannot be seen on the Bermuda long period Columbia vertical but can be read on the Palisades long period Columbia vertical where they show the proper velocities (Fig. 22); (b) a similar situation holds for Hawaiian shocks recorded at Berkeley and Palisades, the former recording short period waves and the latter first mode Rayleigh waves; (c) Mid-Atlantic Ridge shocks on the Bermuda Milne Shaws showing only short period surface waves at the time for R1, show normal first mode waves at the time for R2.

2. In many cases both the first mode Rayleigh waves and the short period surface waves are present, superposed on each other. For example Fig. 5 C, D illustrates this for a shock in the Easter Island region recorded at Honolulu.

3. The short period surface waves show extreme attenuation upon passing a continental boundary and similar but less extreme attenuation for an island arc. However waves of this period range are propagated very efficiently within either oceanic or continental areas. (a) This immediately explains the observations of (1). Because of the differences in character of the continental margins of the Pacific and the Atlantic, Berkeley would be expected to reveal a close approximation to the oceanic train, whereas Palisades is far enough from the continental shelf to record largely continental waves. (b) It likewise explains the fact that Alaskan and west coast shocks make predomin-

antly short period waves at Honolulu only if off shore or very near the coast. (c) Similar effects for microseisms have been suggested by Donn[7]. (d) These ideas are in full agreement with observations on the Lg phase[23]. Lg is a surface shear wave having periods from 1/2 to 6 seconds. It is confined to continental paths. Earthquakes having epicenters only a few degrees offshore do not make this phase at continental stations. The shorter periods are lost as soon as a very small portion of the path is oceanic, whereas the long periods remain until the oceanic segment becomes larger. A reasonable assumption of a value for the phase velocity of these waves and for those of the later part of the short period train gives a very rough value of about 20-35 km for the wavelengths involved. This is also the order of the thickness of the continental crust so that the effects noted here are not unreasonable. Theoretical considerations of the problem of surface waves incident on a boundary representative of the ocean-continent one have never been attempted to the authors' knowledge, and, from a cursory inspection, appear to be somewhat involved.

4. Details at the focus are important factors in determining the excitation ratios for the long and short period surface waves. Depth of focus, topography within a few hundred meters, the initial frequency spectrum of the shock and the geometry of the displacement are relevant.

Greater focal depth clearly discriminates against the shorter waves. In fact, if the usual depths of focus are accepted as correct it is necessary to appeal to topographic effects to account for the presence of appreciable energy in the shorter period surface waves. The principal evidence now available is (a) a few closely neighboring shocks in the Aleutians may produce either long or short period surface waves at Honolulu; (b) in Alaska and in the Fiji Islands there are cases where a shock farther behind the barrier made only short period waves at Honolulu, whereas shocks nearer the open water produced both kinds of waves; (c) as above the earthquakes making short period surface waves tend to group in areas where only normal depth sources are found.

Conclusions

1. The theory attributing most of the dispersion of Rayleigh waves over oceanic paths to the effect of the water layer is confirmed in the Pacific at all azimuths from Honolulu, and over parts of the Atlantic.

2. Love and Rayleigh wave dispersion in the period range studied is in agreement with the crustal structure deduced from refraction shooting. This structure consists of a layer of water and sediments about 5.7 km thick overlying a rock layer of similar thickness and with a compressional wave velocity of about 6.5 km/sec.

This in turn overlies a thick rock layer with compressional velocity of 8.1 km/sec. Poisson's ratio for the rock is 0.27.

3. No submerged land mass of continental character and dimensions exists under the Pacific as outlined by the earthquake belt in Fig. 1, or under parts of the North Atlantic. There is no indication of a submerged Melanesian continent. Limitations of the method, however, prevent the detection of thin layers of continental rock, particularly if they are present over a limited portion of the path.

4. The Easter Island Rise is an anomalous area. Results of this study are in agreement with the theory that a thin layer of continental rock underlies the Easter Island Rise, but are not conclusive evidence.

5. The average thickness of the sedimentary layer in the Pacific is from 0.5 to 1.0 km. The thicker sediments are in the southwest quadrant. A similar range of thicknesses is found in the Atlantic.

6. In addition to the first mode Rayleigh waves and Love waves of the "G" type, some earthquakes make a surface wave of shorter period. These earthquakes have a peculiar geographical distribution, generally occurring in areas where only shallow shocks are known to occur.

7. The first part of the short period train consists of Love waves that fit the first mode Love wave dispersion curve. Consid-

erable effort was spent in an attempt to find a good theoretical explanation for the later part of the train. Although the second mode of the Rayleigh wave solution gives an approximate fit there are significant difficulties. The problem is further complicated by lateral refraction of the shorter wavelengths. There is no good explanation for the later part of the train.

8. There are striking similarities between the late short period waves and long period microseisms, e.g. the periods are identical, particle motion is incoherent, and there is a strong vertical component.

9. The short period waves are sharply attenuated at a continental margin but travel well through continents and oceans alone.

Acknowledgments

The authors wish to thank the U.S. Coast and Geodetic Survey, in particular Mr. Frank Neumann and Mr. L. M. Murphy, for the loan of the Honolulu seismograms and other valuable assistance. Similar acknowledgments are due the Berkeley, Bermuda, Ottawa and Kew stations for the use of their records.

References

1. Brilliant, R. and M. Ewing, "Dispersion of Rayleigh Waves Across the United States", in press, Bull. Seism. Soc. Am.

2. Bullen, K. "An Introduction to the Theory of Seismology", Cambridge University Press (1947).

3. Byerly, P. "The Dispersion of Seismic Waves of the Love Type and the Thickness of the Surface Layer Under the Pacific", Gerlands Beitr. Geophysik, 26: 27-33 (1930).

4. ----------, A.I. Mei, S.J., and Carl Romney, "Dependence on Azimuth of the Amplitudes of P and PP", Bull. Seism. Soc. Am., 39, p. 269 (1949).

5. Carder, D.S., "Seismic Surface Waves and Crustal Structure of the Pacific Region", Bull. Seism. Soc. Am., 24, p. 231 (1934).

6. Coulomb, J., "Love Waves of the Queen Charlotte Islands Earthquake of August 27, 1949", Bull. Seism. Soc. Am., 42, p. 29, January (1952).

6a. Daly, R.A., "Strength and Structure of the Earth", New York (1940).

7. Donn, W.L. "Cyclonic Microseisms Generated in the Western North Atlantic Ocean", Jour. Met. 9: 61-71, February (1952).

8. Evernden, Jack F., "Direction of Approach of Rayleigh Waves and Related Problems", Abstract of paper presented to Geol. Soc. Am. (1952).

9. ---------- "Love Wave Dispersion and the Structure of the Pacific Basin", Abstract of paper presented to Geol. Soc. Am. (1952).

10. Ewing, M. and F. Press, "Crustal Structure and Surface Wave Dispersion, Part I", Bull. Seism. Soc. Am., 40, 4: 271-280 (1950).

11. ----------, "Propagation of Earthquake Waves Along Oceanic Paths", Travaux Scientifiques, 18, Bureau Central Seismologique International (1952).

12. Ewing, M. and F. Press, "Crustal Structure and Surface Wave Dispersion, Part II", Bull. Seism. Soc. Am., 42, 4: 315-325 (1952).

13. ---------, et al., "Seismic Refraction Measurements in the Atlantic Ocean Basin,, Part I", Bull. Seism. Soc. Am., 40, 3: 233-242, July (1950).

14. ---------- and F. Press, "An Investigation of Mantle Rayleigh Waves", in press, Bull. Seism. Soc. Am.

15. Gutenberg, B. and C.F. Richter, "On Seismic Waves" (3rd paper), Gerlands Beitr. Geophysik, 47: 73-131 (1936).

16. ----------, "Seismicity of the Earth", Geol. Soc. Am. Spec. Paper 34 (1941).

17. ----------, "Internal Constitution of the Earth", Dover Publications Inc. (1951).

18. Jardetzky, W.S. and Frank Press, "Crustal Structure and Surface Wave Dispersion, Part III", in press, Bull. Seism. Soc. Am.

19. Neumann, F., "The Velocity of Seismic Surface Waves over Pacific Paths", Bull. Seism. Soc. Am., 19, p. 63 (1929).

20. Officer, C.B. et al., "Seismic Refraction Measurements in the Atlantic Ocean Basin, Part IV", Bull. Geol. Soc. Am., 63: 777-808, August (1952).

21. Pekeris, C.L., "Theory of Propagation of Explosive Sound in Shallow Water", Geol. Soc. Am. Memoir 27.

22. Press, F., M. Ewing and I. Tolstoy, "The Airy Phase of Shallow Focus Submarine Earthquakes", Bull. Seism. Soc. Am., 40, p. 111 (1950).

23. ----------, "Two Slow Surface Waves Across North America", Bull. Seism. Soc. Am., 42, p. 219 (1952).

24. Raitt, R.W., "Reflection and Refraction of Explosive Waves by the Sea Bottom", Quarterly Progress Report, Marine Physical Laboratory of the Scripps Institution of Oceanography, April-June (1951).

25. Rothe, J. P., "The Structure of the Bed of the Atlantic Ocean", Trans. A. G. U., 32, June (1951).

26. Sezawa, K. and K. Kanai, "Discontinuity in the Dispersion Curve of Rayleigh Waves", Bull. Earth. Res. Inst. Tokyo, 13, p. 237 (1935).

27. Stoneley, R., "The Effect of the Ocean on Rayleigh Waves", Mon. Not. Roy. Astron. Soc., Geophys. Suppl., 1: 349-356 (1926).

27a. Umbgrove, J. H. F., "The Pulse of the Earth", The Hague (1947).

28. Wilson, J. T., "The Love Waves of the South Atlantic Earthquake of August 28, 1933", Bull. Seism. Soc. Am., 30: 273-301 (1941).

29. ---------- and O. Baykal, "Crustal Structure of the North Atlantic Basin as Determined from Rayleigh Wave Dispersion", Bull. Seism. Soc. Am., 38: 41-53 (1948).

TABLE 1

Shocks Recorded at Honolulu

No.	Date Day	Month	Year	Hour GCT	Lat.	Long.	Depth in km	Mag.	Surface Wave Train	Location	G	Δ in km	Δ Cont. in km
1	1	Apr.	46	12 29 04	58°N	162.7°W	50±		S.P.	off Alaska Peninsula			
2	10	Nov.	46	17 43 00	7.8°S	77.8°W			L.P.	Northern Peru	?	9300	330
4	2	Apr.	47	05 39 46	1.8°S	138.3°E			L.P.	Pacific Ocean N. of New Guinea	No	7380	
5	13	June	47	20 24 51	19°N	146°E			L.P.	400 mi. N. of Guam	No	5880	
6	19	June	47	07 34 39	21.7°N	145°E			L.P.	600 mi. N. of Guam	Weak	5820	
7	15	Oct.	47	02 09 45	64.5°N	148.8°W			L.P., S.P.	400 mi. SW of Fairbanks	No	4860	
8	1	Nov.	47	14 58 54	10.8°S	74.5°W			L.P.	150 mi. NE of Lima	Yes	9720	
8a	14	Jan.	48	02 25 36	8.9°S	108.7°W			S.P.	1200 mi. N. of Easter Isl.			
9	24	Jan.	48	17 46 46	10.8°N	121.9°E			L.P.	Philippines	Yes	8570	
10	3	Mar.	48	09 09 54	18 1/2°N	119°E	Norm	7.2	L.P.	Philippines	Yes	8600	390
11	13	Mar.	48	20 02 35	1 1/2°N	126 1/2°E	60	7.1	L.P.	Molucca Passage	Yes	8460	

TABLE 1 (Cont.)

No.	Date Day	Month	Year	Hour GCT	Lat.	Long.	Depth in km	Mag.	Surface Wave Train	Location	G	Δ in km	Δ Cont. in km
12	14	May	48	22 31 49	54.7°N	160.2°W			L.P., S.P. ?	N. Pacific Ocean off Alaskan Peninsula	Possibly		
13	28	June	48	07 13 30	36 1/2°N	136°E	Norm	7.3	L.P.	Honshu, Japan	Yes	6540	610
14	2	Sept.	48	23 34 50	10°N	125 1/2°E	Norm	7.0	L.P.	Philippines	Yes	8240	
15	8	Sept.	48	15 09 14	21.0°S	174.2°W			L.P.	Tonga Region	Weak	5020	
16	10	Sept.	48	13 48 34	43 1/2°N	147°E	40	7.1	L.P., S.P.	Pacific Ocean E. of Hokkaido, Japan	No	5620	
17	16	Mar.	49	22 15 13	5 1/2°S	151°E	60	7.1	L.P.	New Britain Isl.	No.	6320	390
18	17	Mar.	49	21 05 03	5 1/2°S	151°E	60	7.0	L.P.	New Britain Isl.	No.	6320	
19	24	Mar.	49	20 56 58	41.9°N	124.8°W			S.P.	Pacific Ocean off N. Calif. Coast		3850	
20	27	Mar.	49	06 34 05	3 1/2°N	127 1/2°E	Norm	7.0	L.P.	S. of Mindanao	No	8280	
20a	13	Apr.	49	19 55 40	47.1°N	122.6°W			L.P., S.P.	Pacific Northwest	No	4280	
21	20	Apr.	49	03 29 0	38°S	72 1/2°W	70-100	7 1/2	L.P.	Chile	No		
22	2	July	49	19 57 13	16°N	148°E	50	7.2	L.P.	Marianas	No	5710	
23	5	Aug.	49	19 08 47	1°S	78°W			L.P.	Central Ecuador	No	8990	280

TABLE 1 (Cont.)

No.	Date Day	Month	Year	Hour GCT	Lat.	Long.	Depth in km	Mag.	Surface Wave Train	Location	G	Δ in km	Δ Cont. in km
24	14	Sept.	49	19 50 20	3/4°N	126°E	50?	7.2	L.P.	Celebes Region	Yes	8550	450
25	27	Sept.	49	15 30 43	60°N	149°W		7	L.P., S.P.	S. Alaska	Possibly	4370	
26	27	Nov.	49	08 42 16	18°S	173°W			L.P.	Tonga Isl. Region	Possibly	4660	
27	17	Dec.	49	15 07 53	54°S	71°W		7 1/2, 7 1/4	L.P.	Punta Arenas	Yes	1170	
27a	17	Dec.	49	06 53 29	54°S	71°W			L.P.	Punta Arenas	Yes		
28	29	Dec.	49	03 03 55	18 1/2°N	121°E	Norm	7.2	L.P.	N. Tip of Luzon	No	8400	
29	17	May	50	18 13 13	21°S	169°E	40	7.0		New Hebrides		5830	
30	25	May	50	18 35 00	13°N	142 1/2°E	100	7 1/4 Pas	L.P.	150 mi. W. of Guam	Yes	6370	
31	24	June	50	22 25 34	20 1/2°S	169 1/2°E	40	7.2	L.P.		Weak	8340	
31a	25	June	50	11 05 51	5°N	127°E		6 1/2	L.P.	S. of Mindanao	Weak	8270	
31b	29	July	50	14 36 33	33°N	115 1/2°W			S.P.			4360	
32	31	Aug.	50	07 05 35	6°N	126°E		7	L.P.	Off S. coast of Mindanao	Weak	8340	
33	29	Sept.	50	06 32 14	19°N	107°W		7	S.P.	Off Colima	Yes	5300	

TABLE 1 (Cont.)

No.	Date Day	Month	Year	Hour GCT	Lat.	Long.	Depth in km	Mag.	Surface Wave Train	Location	G	in km	Cont. in km
33a	4	Oct.	50	00 41 07	18 1/2°S	170°E			L. P.	New Hebrides	No	5640	
34	5	Oct.	50	16 09 31	11°N	85°W	Norm	7.7	L. P., S. P. ?	Costa Rica	Yes	7840	
35	5	Nov.	50	17 37 27	33 1/4°N	134 3/4°E	Norm	6.9	L. P.	Japan	Yes	6700	
36	8	Nov.	50	02 18 12	10°S	159 1/2°E	Norm	7 1/4	L. P., S. P. ?	Solomons	Yes	5810	
37	17	Nov.	50	19 28 18	17°N	100 1/2°W	6	3/4-7	L. P.	Near west coast of Mexico	No.	6010	
38	5	June	51	16 57 47	30°N	132°E	100	6 3/4-7	L. P.	S. of Kyushu	No	7000	
40	17	June	51	23 46 58	44 1/2°N	130°W		5 1/2	S. P.	300 mi. off coast of Oregon		3640	
41	8	July	51	05 44 20	11°N	122°E		6 1/2	L. P.	Panay Isl. Philippines	Yes	8560	400
42	21	Oct.	51	21 34 13	11°N	122°E			L. P.	Formosa	Yes	8120	

TABLE 1 (Cont.)

No.	Date Day	Month	Year	Hour GCT	Lat.	Long.	Depth in km	Mag.	Surface Wave Train	Location	G	Δ in km	Δ Cont. in km
42a	22	Oct.	51	03 29 26	24°N	122°E			L.P.	Formosa	Yes	8120	
42b	22	Oct.	51	05 43 01	24°N	122°E			L.P.	Formosa	no	8120	
43	6	Nov.	51	16 40 06	47°N	154°E			L.P.,S.P.	Kurile Isl.	No	5170	
45	8	Nov.	51	13 45 09	54 1/2°N	160°W		6 1/4	S/P.	Aleutians	Possibly	3710	
46	24	Nov.	51	18 50 19	23°N	121°E		7 1/4	L.P.	Formosa	No	8150	
47	10	Apr.	47	15 58 04	35.0°N	116.6°W			S.P.	Mojave Desert, Calif.		4290	
48	2	May	47	02 19 06	53.8°N	164.3°W	50±		S.P.	N. Pacific Ocean off Unimak Isl.		3690	
49	27	Aug.	47	13 37 48	37.8°	179.1°			S.P.	Off SE coast No. Isl. New Zealand		6990	
50	23	Sept.	47	13 52 58	40.2°N	125.8°W			S.P.	Cape Mendocino, Cal.		3690	
51	20	Oct.	47	01 43 17	64.0°N	147.9°W			L.P.,S.P.	Fairbanks & Mt. McKinley area		4780	
52	2	Nov.	47	07 00 26	40°N	127°W			S.P.	Cape Mendocino, Cal.		3590	
53	21	Nov.	47	03 54 15	19°N	107°W			S.P.	Off Mexico		5290	
54	28	Feb.	48	01 58 05	53.2°N	133.0°W		6 1/2	S.P.	Queen Charlotte Isl.		4170	

TABLE 1 (Cont.)

No.	Date Day	Month	Year	Hour GCT	Lat.	Long.	Depth in km	Mag.	Surface Wave Train	Location	G	Δ in km	Δ Cont. in km
55	14	May	48	22 31 49	54.7°N	160.2°W			S.P.	N. Pacific Ocean off Alaskan Peninsula		3720	
56	17	May	48	17 48 42	54.8°N	160.1°W	75		L.P., S.P.	N. Pacific Ocean off Alaskan Peninsula		3770	
57	26	May	48	19 16 58	55.8°N	152.6°W		6	S.P.	Pacific Ocean off Alaskan Peninsula		3880	
57a	15	July	48	11 02 15	11°N	104°W	100		S.P.	550 mi. W. of Mexico coast		5870	
58	22	July	48	20 05 27	49 1/2°N	130 1/2°W			S.P.	Pacific Ocean W. off Vancouver Isl.		3960	
58a	22	July		20 52 39	50°N	130°W			S.P.	Pacific Ocean W. off Vancouver Isl.		3960	
59	7	Aug.	48	14 40.2	34°N	142°E			L.P., S.P.	Off Honshu Isl., Japan		6020	
60	19	Aug.	48	13 50 52	62.7°N	149.1°W	100	6 1/4	S.P.	Near Anchorage		4540	
60a	30	Dec.	48	23 49 53	51.5°N	130.0°W		6.6	S.P.	Queen Charlotte Isl.		4140	
61	22	Aug.	49	04 01 12	54°N	133°W		7 1/2-8	S.P.	Queen Charlotte Isl.		4140	
62	23	Aug.	49	19 43 35	53°N	132°W		6 1/2	S.P.			4170	
62a	24	Aug.	49	06 07 14	43 1/2°N	127°W			S.P.	West of Oregon		3770	

TABLE 1 (Cont.)

No.	Date Day	Month	Year	Hour GCT	Lat.	Long.	Depth in km	Mag.	Surface Wave Train	Location	G	Δ in km	Δ Cont. in km
62b	24	Aug.	49	09 22 02	9°S	109°W			L.P., S.P.	1200 N. of Easter Isl.		6290	
63	31	Oct.	49	01 39 32	56°N	135°W		6 3/4	S.P.			4310	
64	26	Dec.	49	06 23 54	14 1/2°S	180°E		7	L.P., S.P.	Fiji Isl. Region		4650	
65	10	Jan.	50	03 05 42	11°N	103°W		6 1/4	S.P.	Pacific Ocean off S. Coast of Mexico		5940	
66	12	Feb.	50	22 44 55	19°S	178°E		6.5 pas	S.P.	Fiji Isl. Region		5190	
67	9	July	50	12 34 15	33°S	112°W			S.P.	500 mi. SW of Easter Isl.		7900	
67a	12	July	50	01 36 42	2°N	101°W			S.P.	700 mi. NW of Galapagos		6510	
68	12	July	50	11 09 15	53°N	166°W		6 1/4	S.P.	Aleutian Isl.		3720	
70	22	Sept.	50	07 52 07	25°S	114°W		6.8, 6 1/2	S.P.	Easter Isl. Region		7040	
71	29	Sept.	50	06 32 14	19°N	107°W		7	S.P.	Off Colima		5290	

TABLE 2

Hawaiian Shocks Recorded in North America

No.	Day	Month	Year	Hour	Lat.	Long.	Mag.	Berk.	Surface Waves
A	30	May	50	01 16 16	19 1/2°N	156°W	6 1/4	3830	S. P. (Weak L. P.)
B	23	Apr.	51	00 52 21	19°N	155 1/2°W	6 1/2, 6	3830	S. P.
C	21	Aug.	51	10 56 57 1/2	19 3/4°N	156°W	6 3/4, 7		S. P. (Fresno & Columbia)
D	22	Aug.	51	08 47 51	19 3/4°N	156°W			S. P. (Fresno)

TABLE 3

Atlantic Shocks

No.	Day	Month	Year	Hour	Lat.	Long.	Depth	Mag.	Surface Waves Berm.	Surface Waves Pal.	Location	Δ Berm.	Δ Pal
1	9	Mar.	50	10 03 39*	16°N	60°W			S. P.		Leeward Isl	1880	3090
2	20	May	50	09 37 27*	29°N	43 1/2°W			S. P.	L. P.	N. Atlantic	2050	3050
4	23	July	50	23 32 28*	21°N	64°W			S. P.		200 mi. N. of Puerto Rico	1260	2410
4a	25	July	50	18 15 00*	31°N	42°W				L. P.	Mid Atlantic Ocean		3000
5	26	July	50	08 31 28**					S. P.		Off E. Coast Dominican Republic		
6a	6	Oct.	50	08 16 02	20°N	66°W			S. P.	L. P.	Off Coast Northern Puerto Rico	1380	2440
6b	28	Oct.	50	16 40 36*	32°N	41°W				L. P.	Mid Atlantic Ocean		2970
7	19	Oct.	50	03 48 25	19°N	68°W			S. P.	L. P.	Off NE Coast of Puerto Rico	1490	2670
7a	20	Oct.	50	07 44 30	19°N	68°W			S. P.	L. P.	Off NE Coast of Puerto Rico	1490	2670
7b	31	Oct.	50	19 15 22*	1°N	26°W				L. P.	Mid Atlantic Ocean		6450
8	1	Dec.	50	14 51 00*	14°N	47°W	100	7 1/4-7.4	S. P. (off scale)		Mid Atlantic 800 mi. off NE Coast of Brazil	2720	3990
9	29	Dec.	50	20 16 29*	17°N	63°W	100		S. P., L. P., L. P.		Leeward Isl.	1720	2890

TABLE 3 (Cont.)

No.	Date Day	Month	Year	Hour	Lat.	Long.	Depth	Mag.	Surface Waves Berm	Pal.	Location	Δ Berm.	Δ Pal.
10	30	Jan.	51	19 00 30*	15 1/2°N	99°W		6 1/4-6 1/2	S.P., L.P.		Off S. coast of Mexico	3940	3660
11	31	Jan.	51	11 51 46*	21°N	46°W			S.P.		N. Atlantic Ocean	2240	3440
12	19	Mar.	51	03 07 31*	35 1/2°N	35°W			S.P.		N. Atlantic Ocean	2750	3440
15	27	May	51	04 30 55*	23 1/2°N	45°W			S.P.	L.P.	N. Atlantic Ocean	2160	3250
16	18	July	51	09 06 16	1°N	27°W		6 1/2-6 1/4	S.P. L.P. on R2	L.P.	Mid Atlantic Ocean	5260	6400
17	10	Aug.	51	05 32 33*	8 1/2°N	40°W	6		S.P.		Atlantic Ocean	3680	4900
18	8	Sept.	51	06 42 40*	29°N	43 1/2°W			S.P.	L.P.	N. Atlantic Ocean	1870	3000
19	22	Sept.	51	23 40 37*	16 1/2°N	47°W			S.P. (hint of S.P.)	L.P.	N. Atlantic Ocean	2500	3780
20	3	Oct.	51	02 00 06*	16 1/2°N	61°W			S.P.		Leeward Isl.	1810	3110
21	12	Nov.	51	09 36 36*	17°N	61°W			S.P.		Leeward Isl	1750	2950
22	30	Nov.	51	07 51 17*	32°N	41°W			S.P.		N. Atlantic Ocean	2228	3050
26	19	Jan.	52	06 25 51**					L.P.		700 mi. N. of Azores		
27	23	Feb.	52	21 35 65**	29°N	43°W			S.P.		N. Atlantic Ocean		
28	1	May	52	16 10 41*	28°N	43 1/2°W			L.P., S.P.		N. Atlantic Ocean		

TABLE 4

Constants Used in Calculations of Theoretical Curves

Case	I	II	III
V *	1.52 km/sec	1.52	1.52
α_2	5.5	7.90	6.9
α_3	8.1	---	8.1
H_2	$=H_1$	$=\infty$	$=H_1$
ρ_2	$2.67\rho_1$	$3.0\rho_1$	$2.67\rho_1$
ρ_3	$3.0\rho_1$	---	$3.0\rho_1$
σ	1/4	1/4	1/4

* See p. 9 for definition of symbols.

TABLE 5

Computed Points on Second Mode Rayleigh Wave Dispersion Curve

c/α_o	kH	c/α_o	kH	c/α_o	kH
1.20	6.944	2.00	2.620	2.73	1.265
1.30	5.558	2.05	2.530	2.75	1.173
1.40	4.701	2.10	2.447	2.77	1.079
1.50	4.115	2.20	2.289	2.80	.947
1.60	3.677	2.30	2.144	2.83	.842
1.65	3.495	2.40	2.006	2.85	.789
1.70	3.333	2.50	1.862	2.875	.738
1.75	3.187	2.55	1.777	2.90	.700
1.80	3.054	2.60	1.680	2.95	.646
1.85	2.932	2.65	1.555	3.00	.608
1.90	2.820	2.70	1.389	3.0766	.557
1.95	2.716				

TABLE 6

Compressional and Shear Wave Velocities Corresponding to Various Values of Poisson's Ratio

σ	α	β	α	β	α	β	α	β
.23	8.1	4.80	7.9	4.68	6.9	4.09	6.5	3.85
.25	8.1	4.68	7.9	4.56	6.9	3.98	6.5	3.75
.27	8.1	4.55	7.9	4.43	6.9	3.87	6.5	3.65
.28	8.1	4.48	7.9	4.37	6.9	3.81	6.5	3.59
.30	8.1	4.33	7.9	4.22	6.9	3.69	6.5	3.47

TABLE 7

Liquid,* Water, and Sediment Thickness for Atlantic Shocks

No.	Day	Month	Year	Recording Station	Liquid	Water	Sediment
4A	25	July	50	Palisades	5.3 km	4.8 km	0.5 km
6B	8	Oct.	50	Palisades	5.3 km	4.8 km	0.5 km
6B	8	Oct.	50	Palisades	5.3 km	4.8 km	0.5 km
7B	31	Oct.	50	Palisades	5.1 km	4.0 km	1.1 km
8	1	Dec.	50	Palisades	5.5 km	4.9 km	0.6 km
8	1	Dec.	50	Ottawa	5.5 km	4.9 km	0.6 km
8	1	Dec.	50	Kew	4.8 km	4.2 km	0.6 km

* Liquid = water + sediment

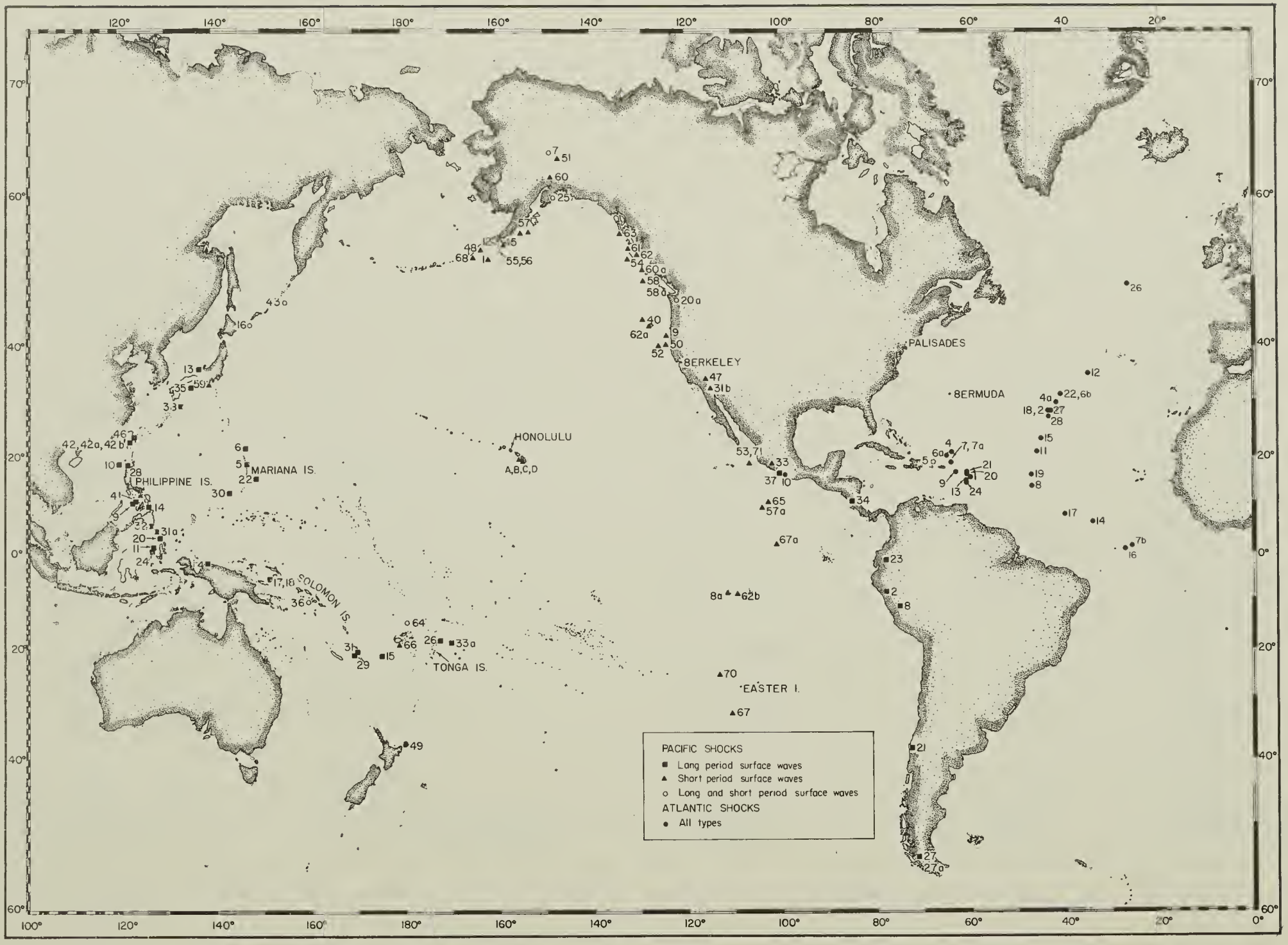

Figure 1. Map of Epicentral Locations of Selected Earthquakes

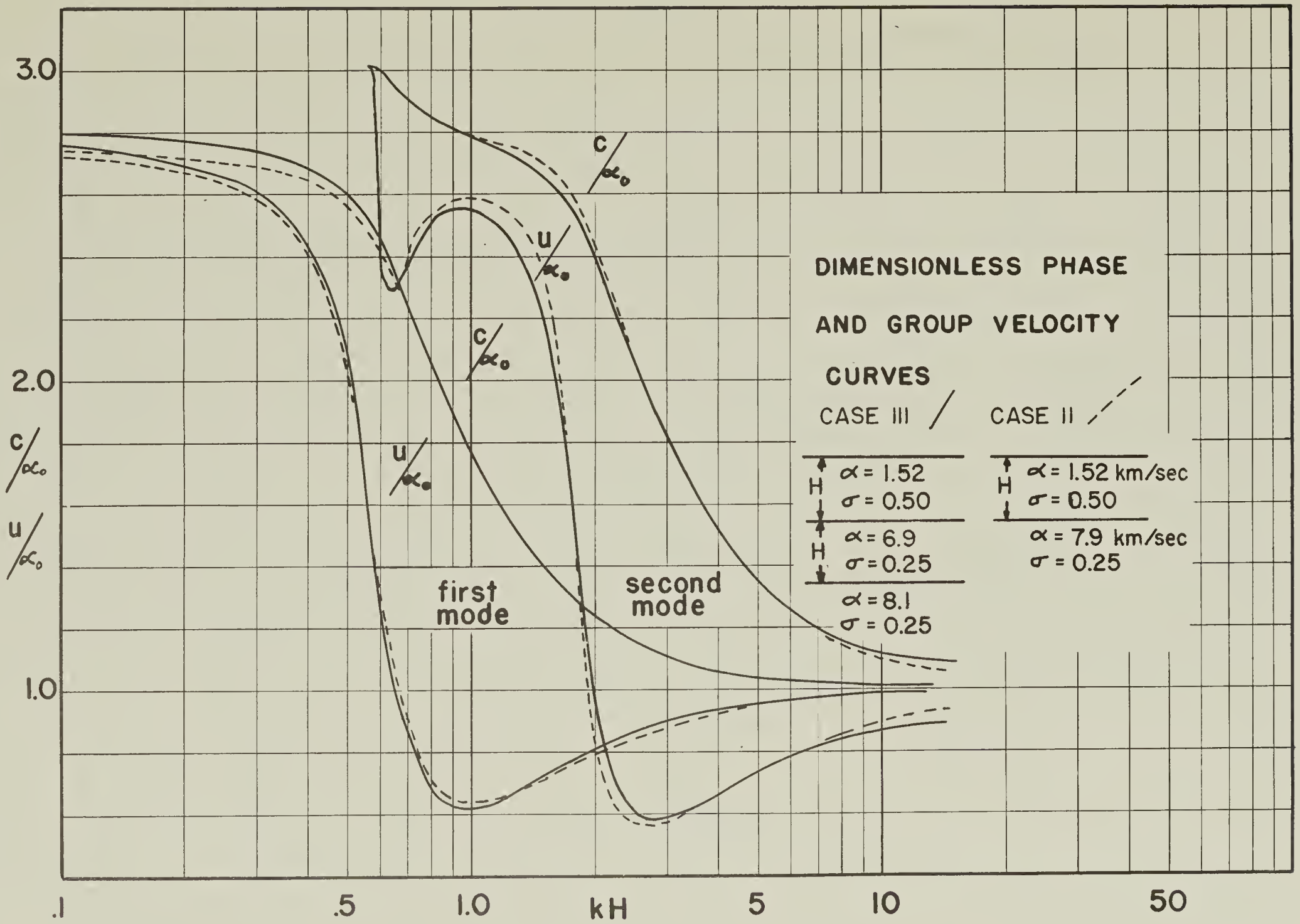

Figure 2. Dimensionless Phase and Group Velocity, First and Second Modes

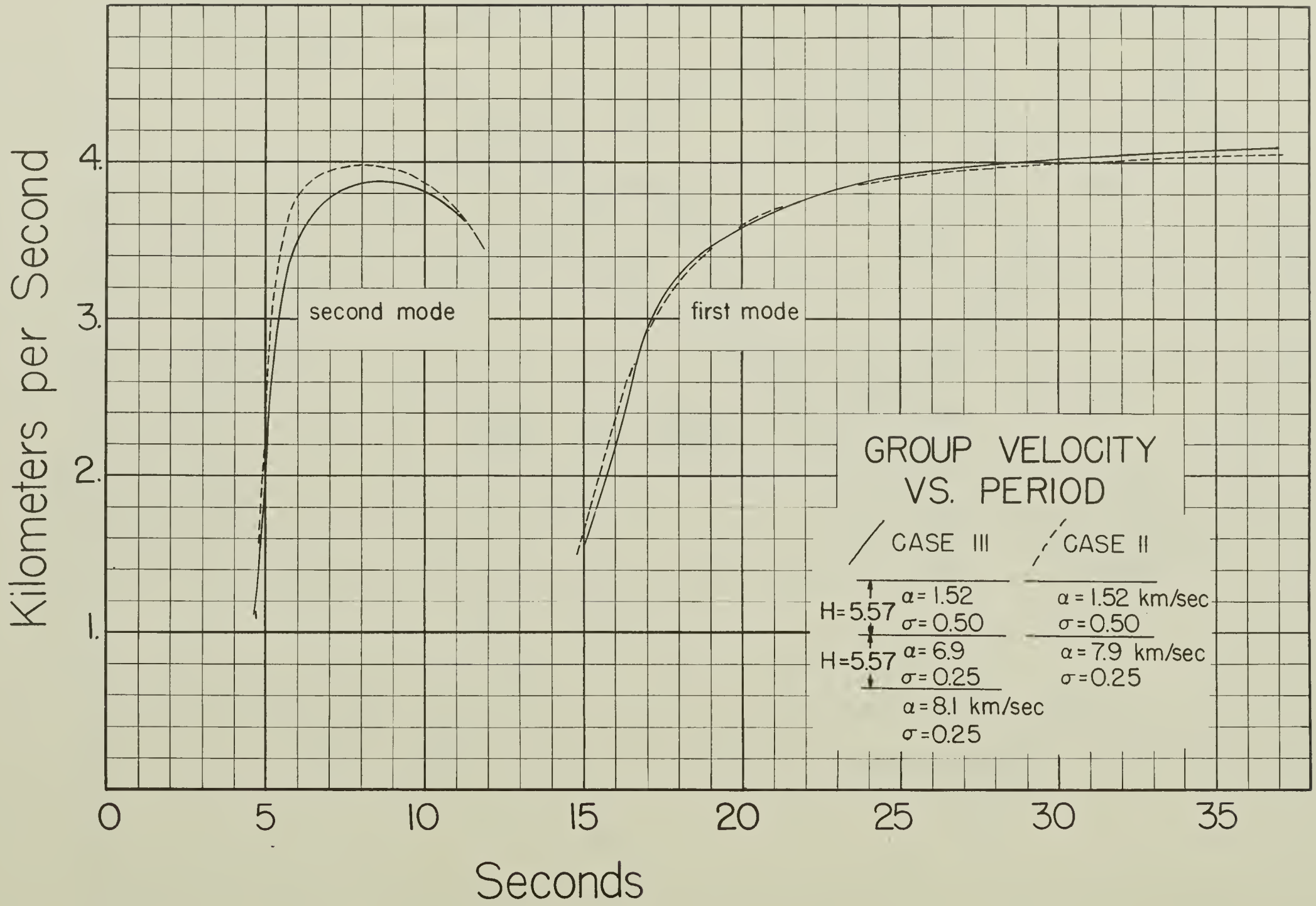

Figure 3. Group Velocity, First and Second Modes, Dimensions Pertinent to Earthquakes

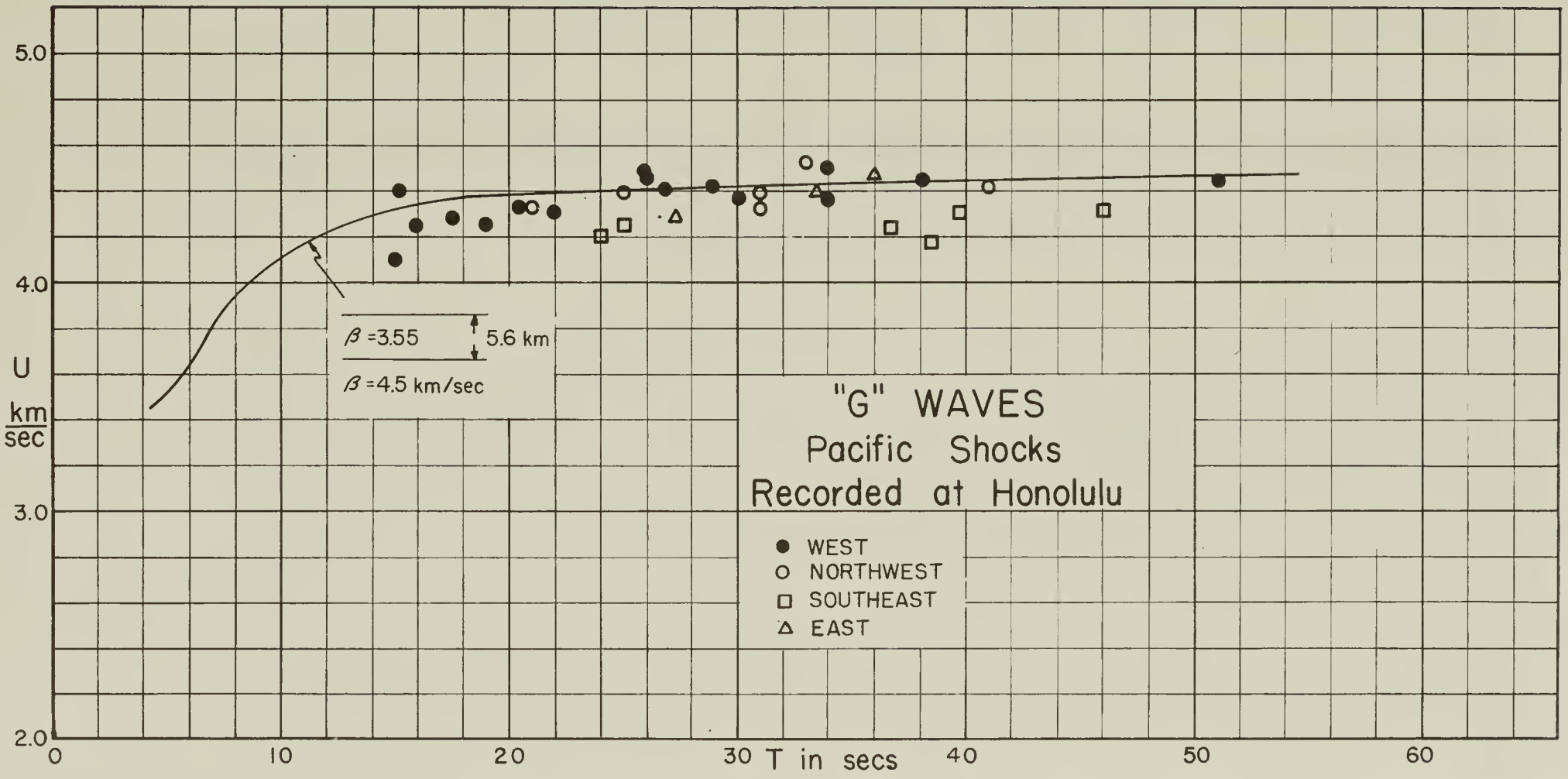

Figure 4. "G" Waves

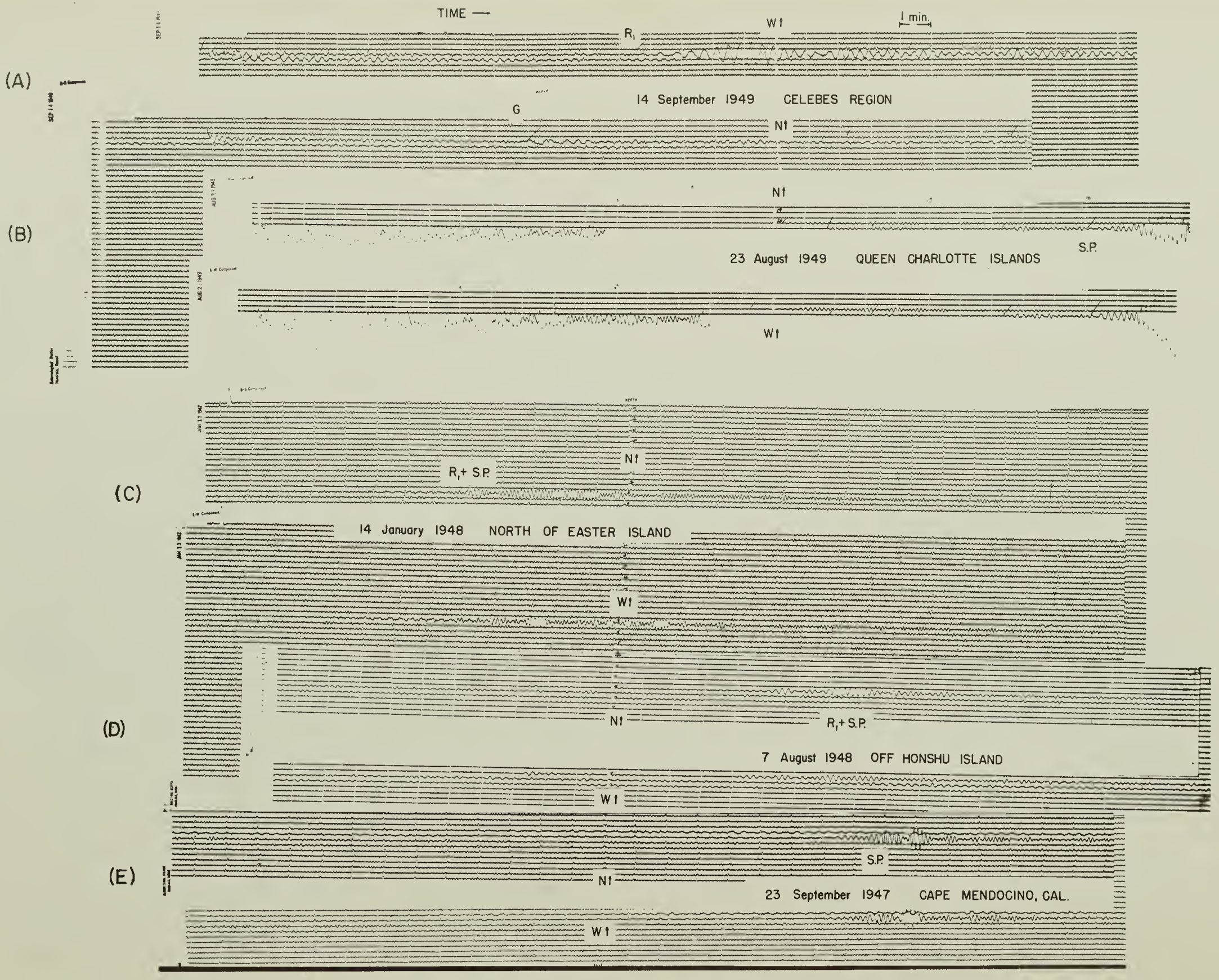

Figure 5. Seismograms

A First Mode Rayleigh and Love Waves

B, E Short Period Surface Waves

C, D Mixed Long and Short Period Surface Waves

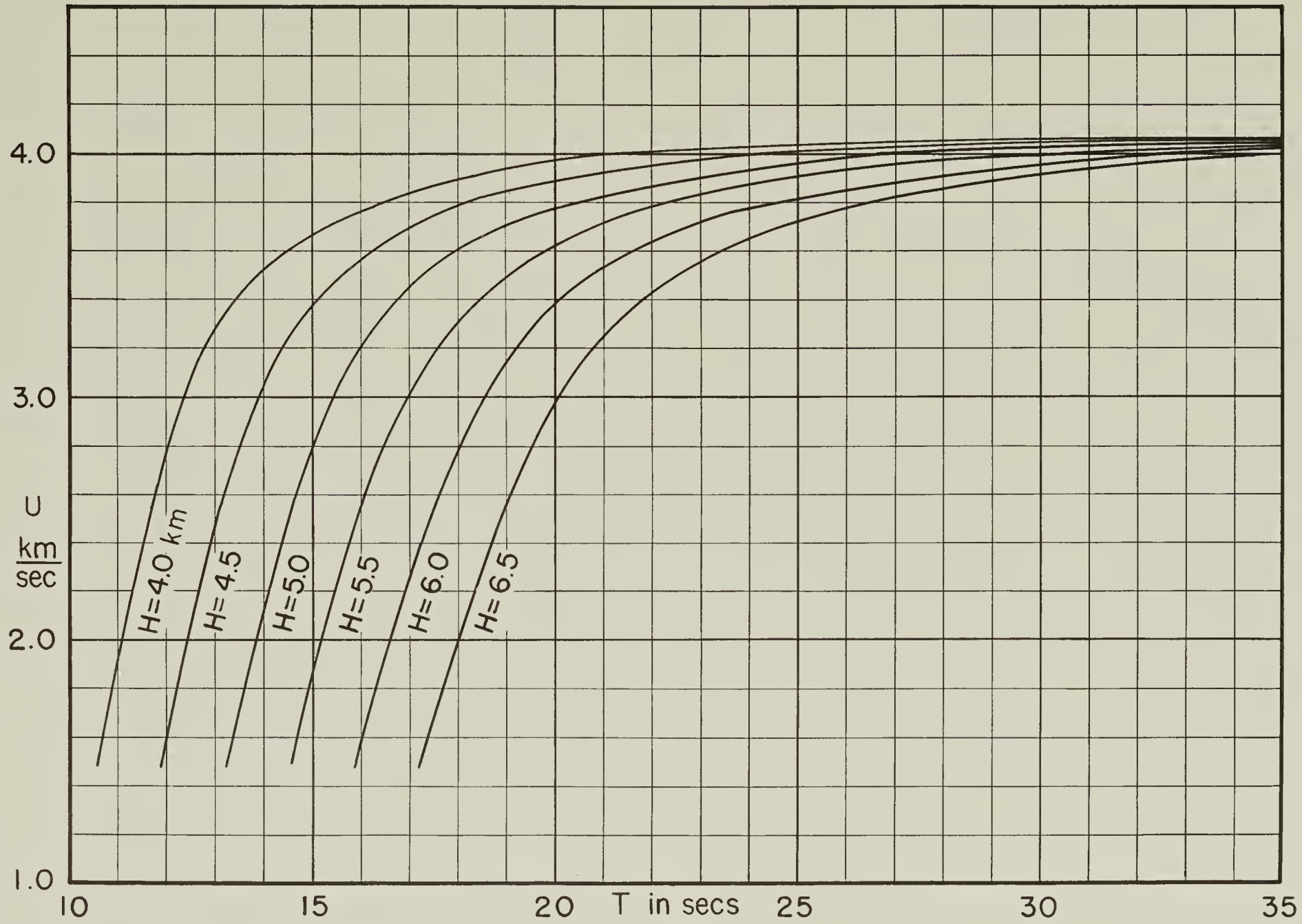

Figure 6. Dependence of Rayleigh Waves on Liquid Depth

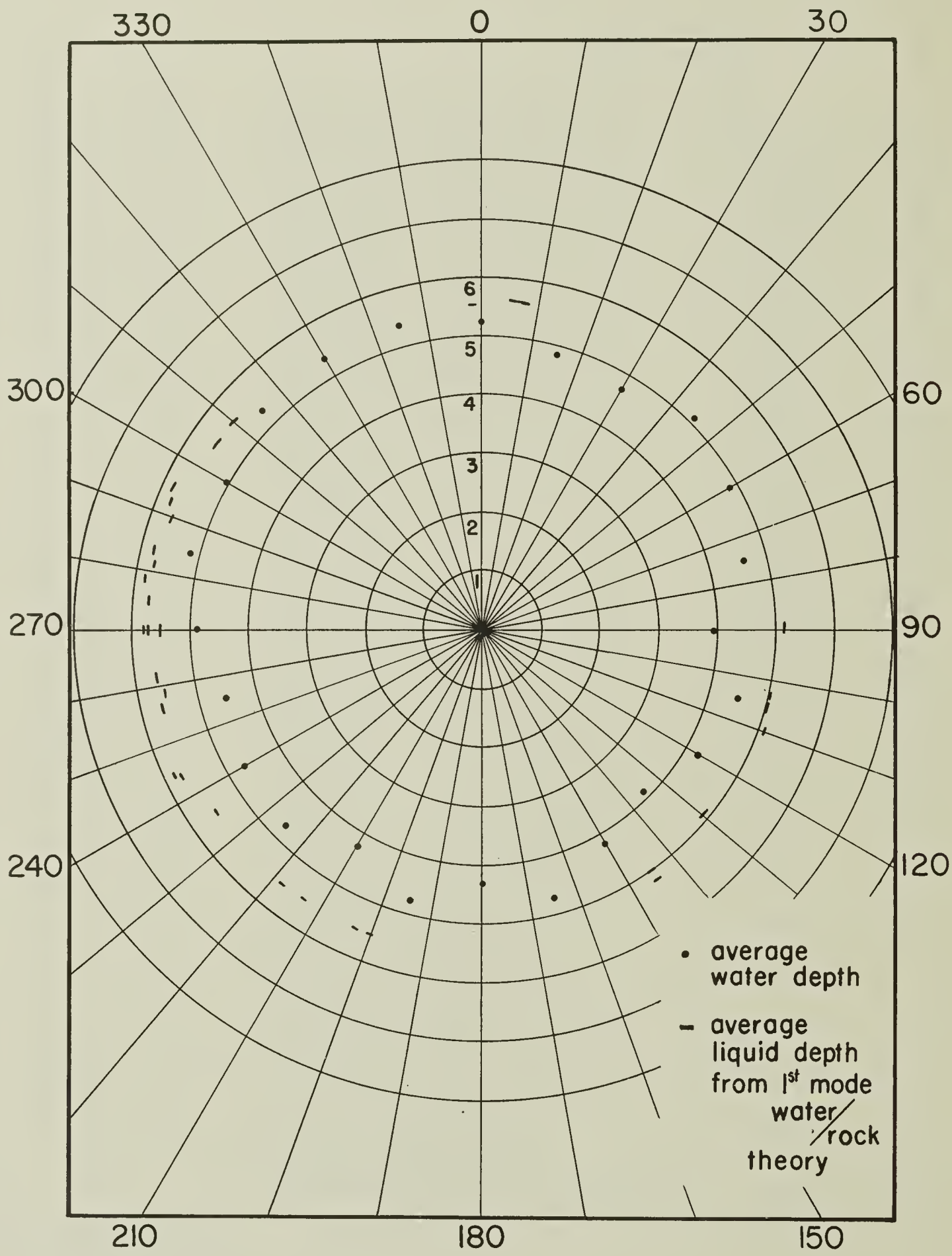

Figure 7. Sediment Thicknesses in the Pacific
(Sediment Thickness = Liquid Depth - Water Depth)

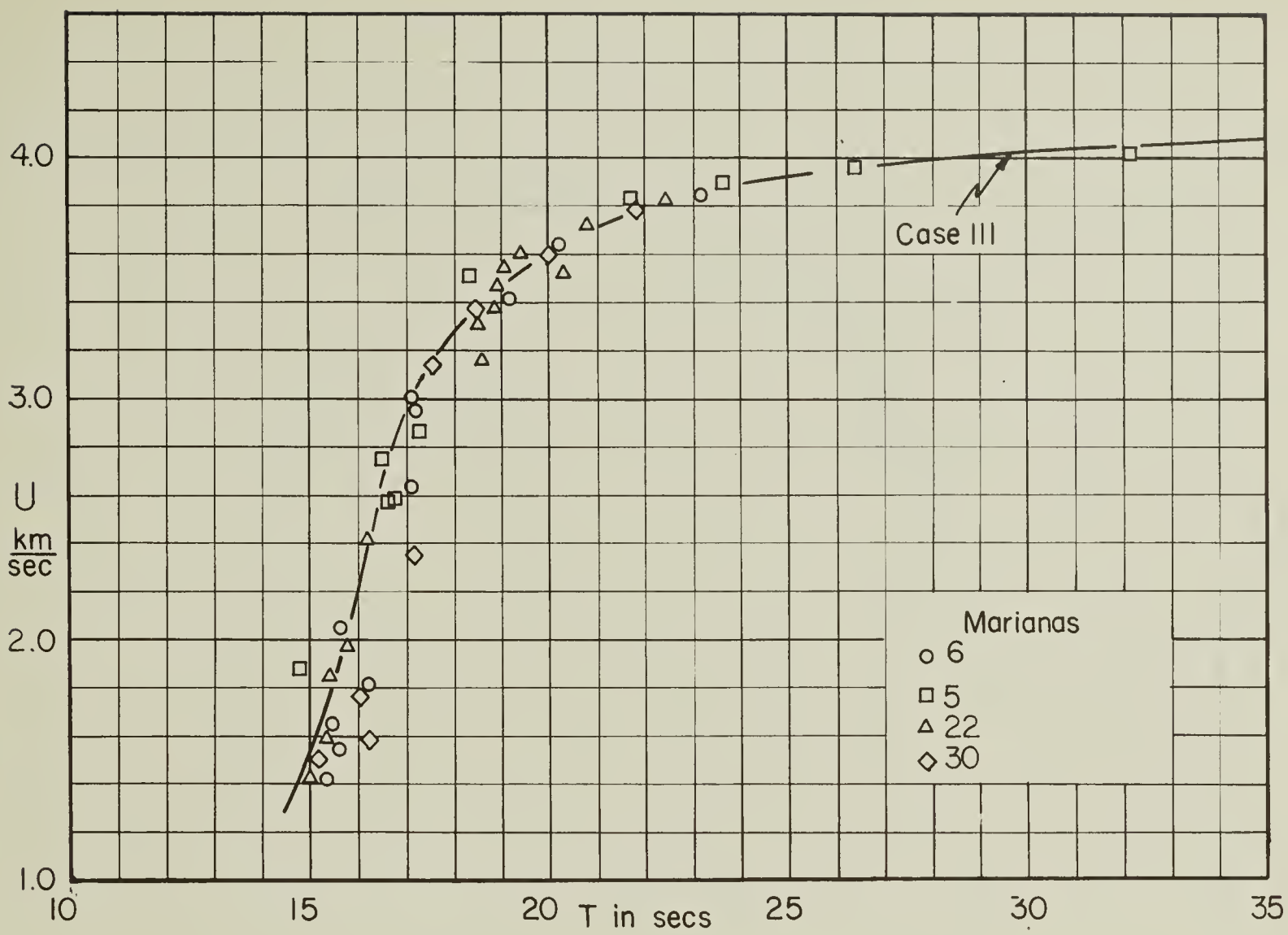

Figure 8. Rayleigh Wave Dispersion, Marianas (Table 1)

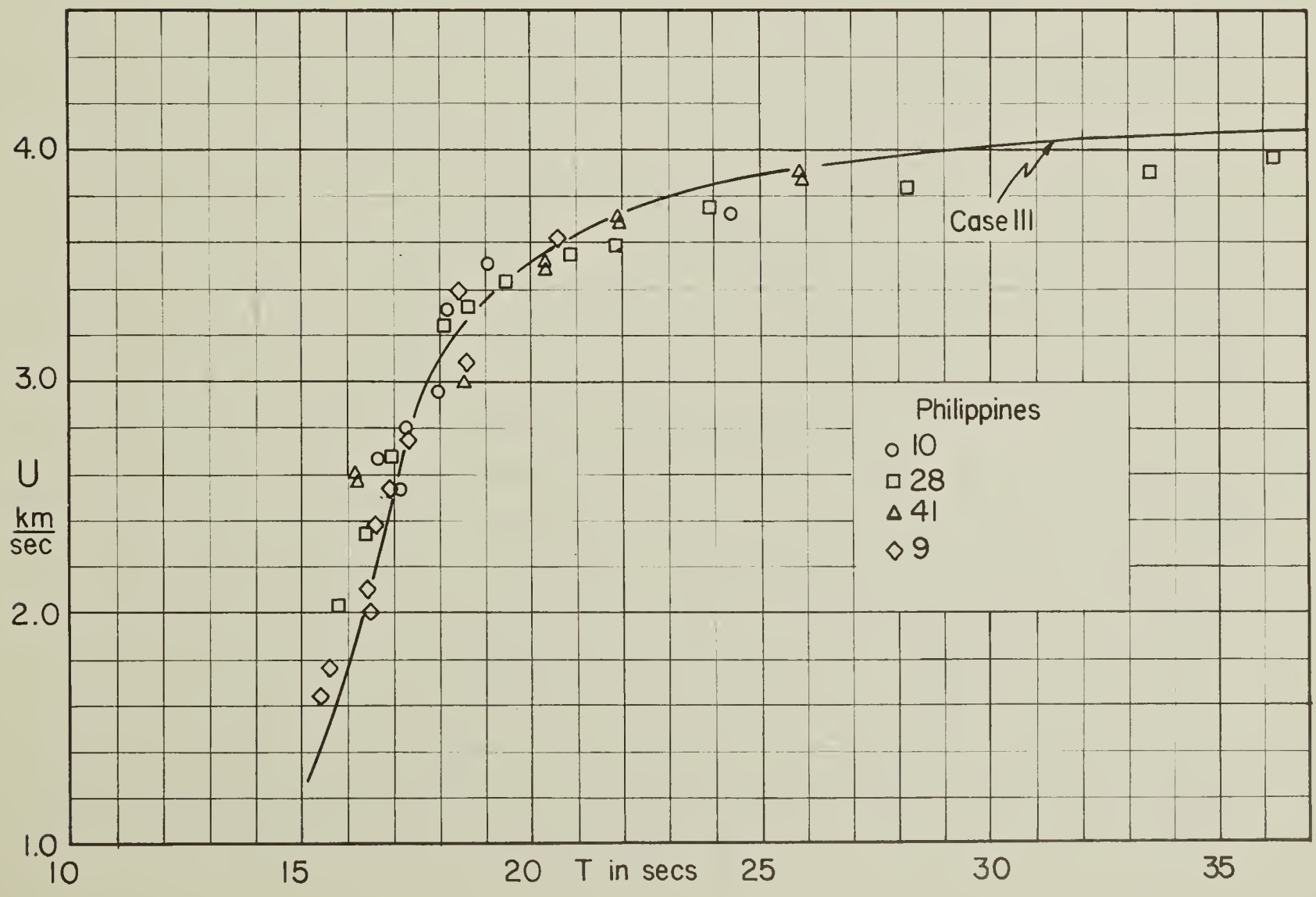

Figure 9. Rayleigh Wave Dispersion, Philippines (Table 1)

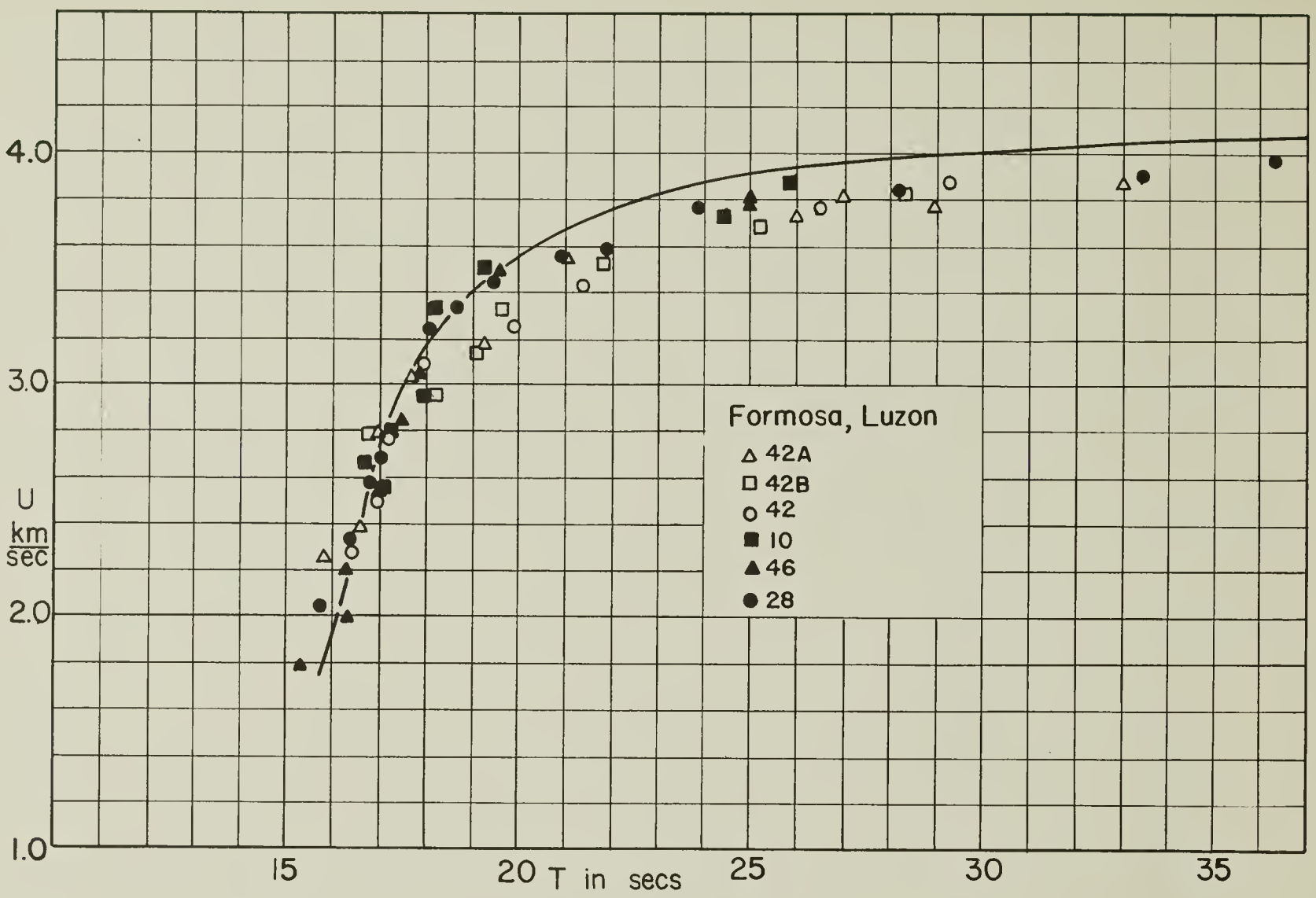

Figure 10. Rayleigh Wave Dispersion, Formosa, Luzon (Table 1)

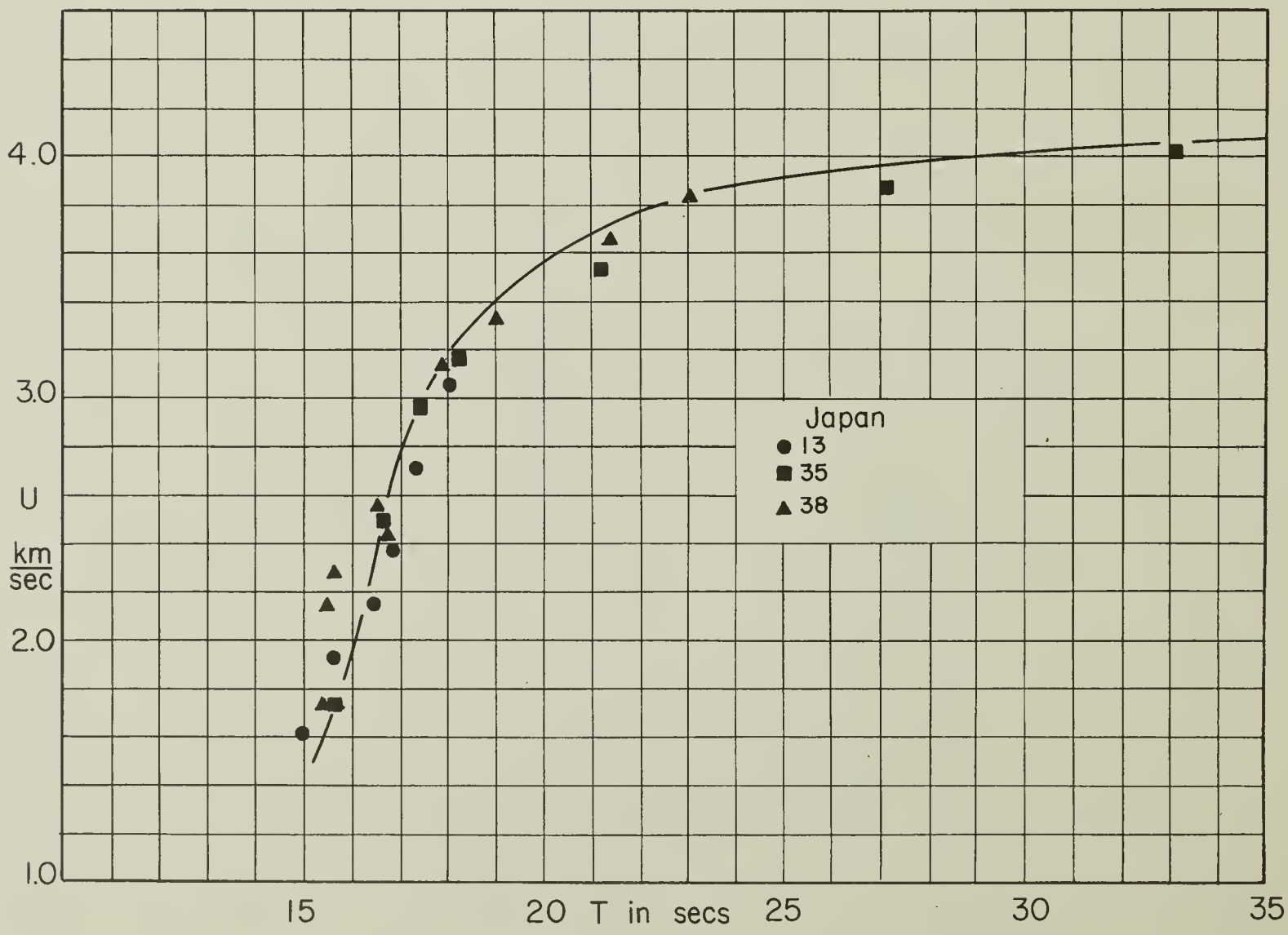

Figure 11. Rayleigh Wave Dispersion, Japan (Table 1)

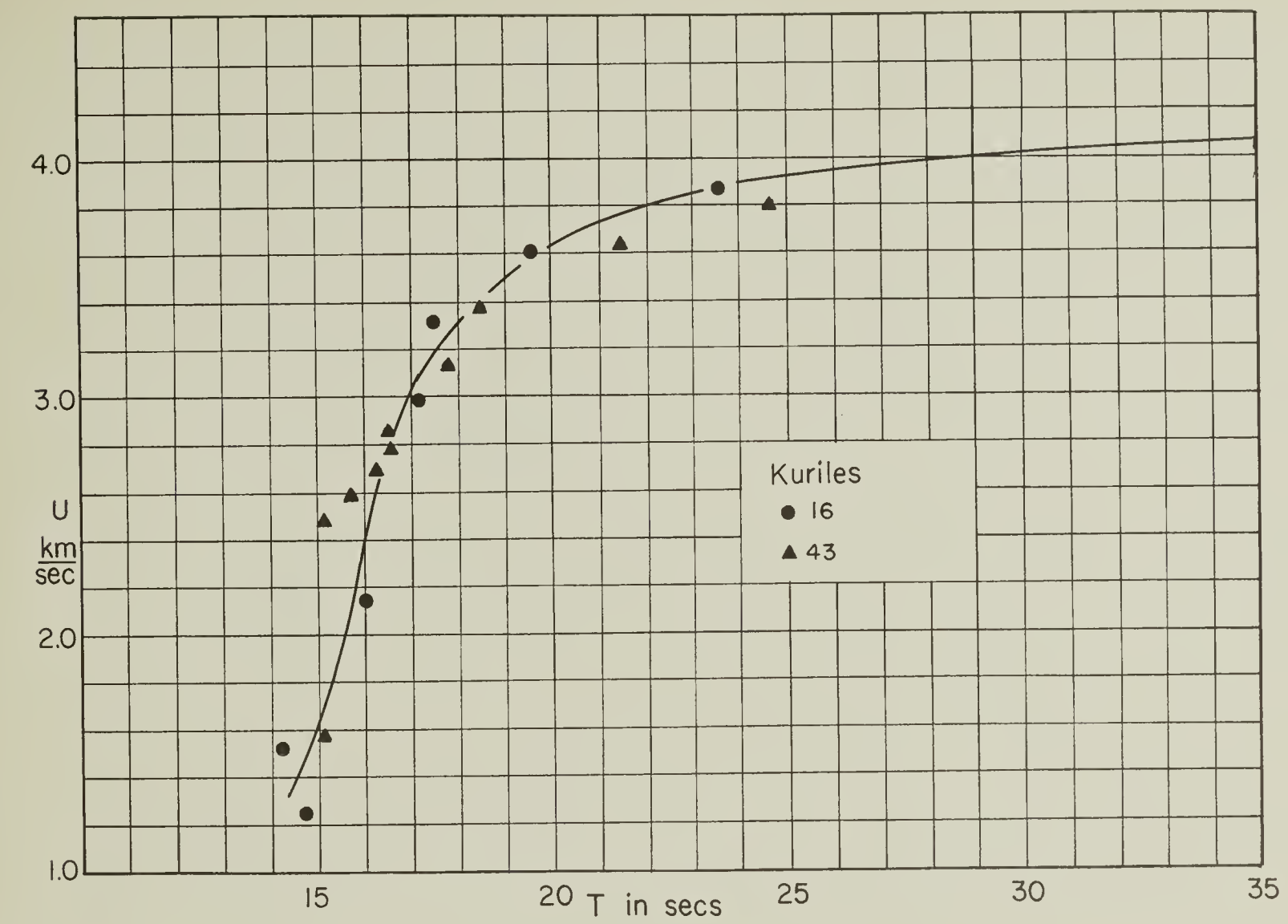

Figure 12. Rayleigh Wave Dispersion, Kuriles (Table 1)

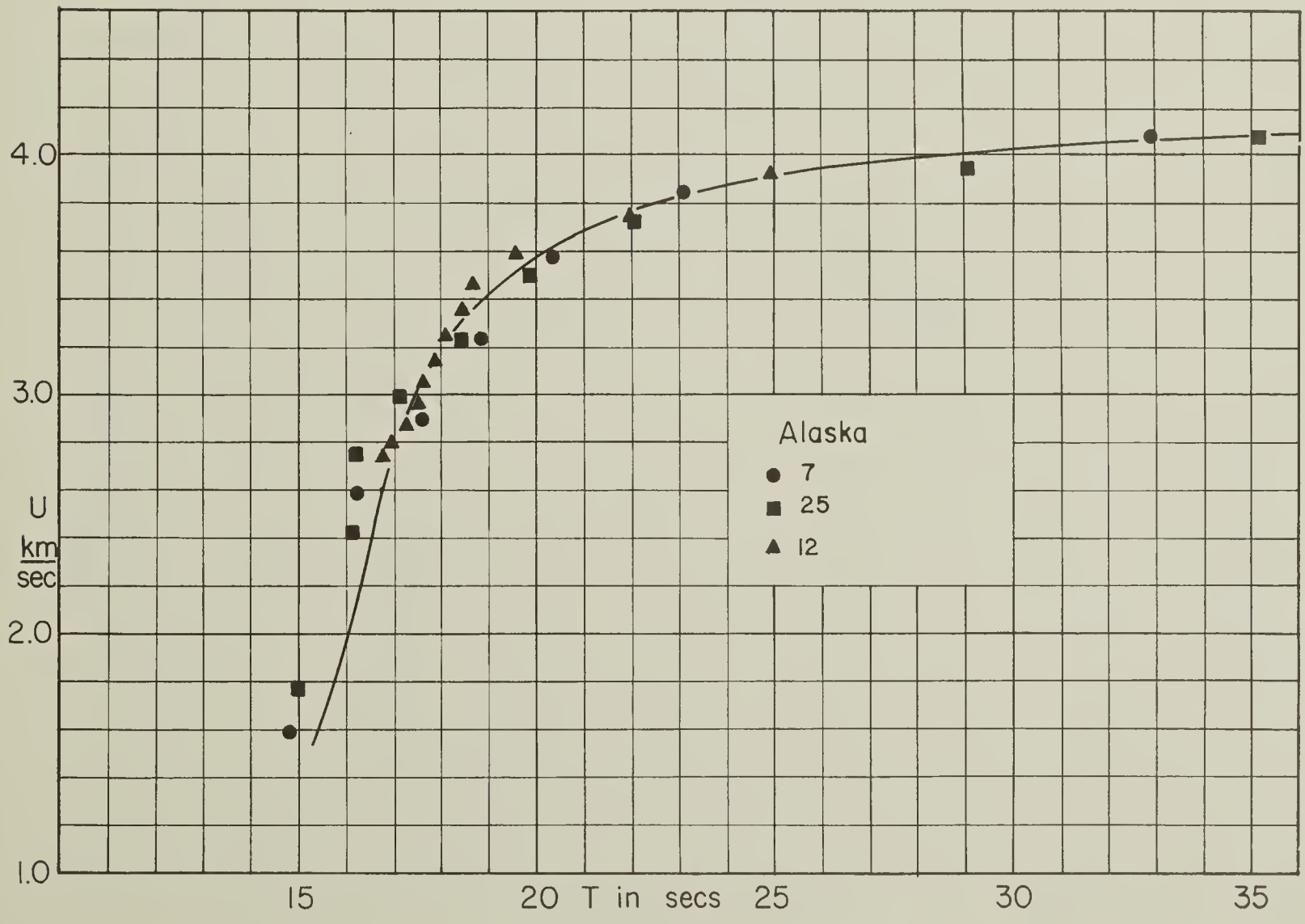

Figure 13. Rayleigh Wave Dispersion, Alaska (Table 1)

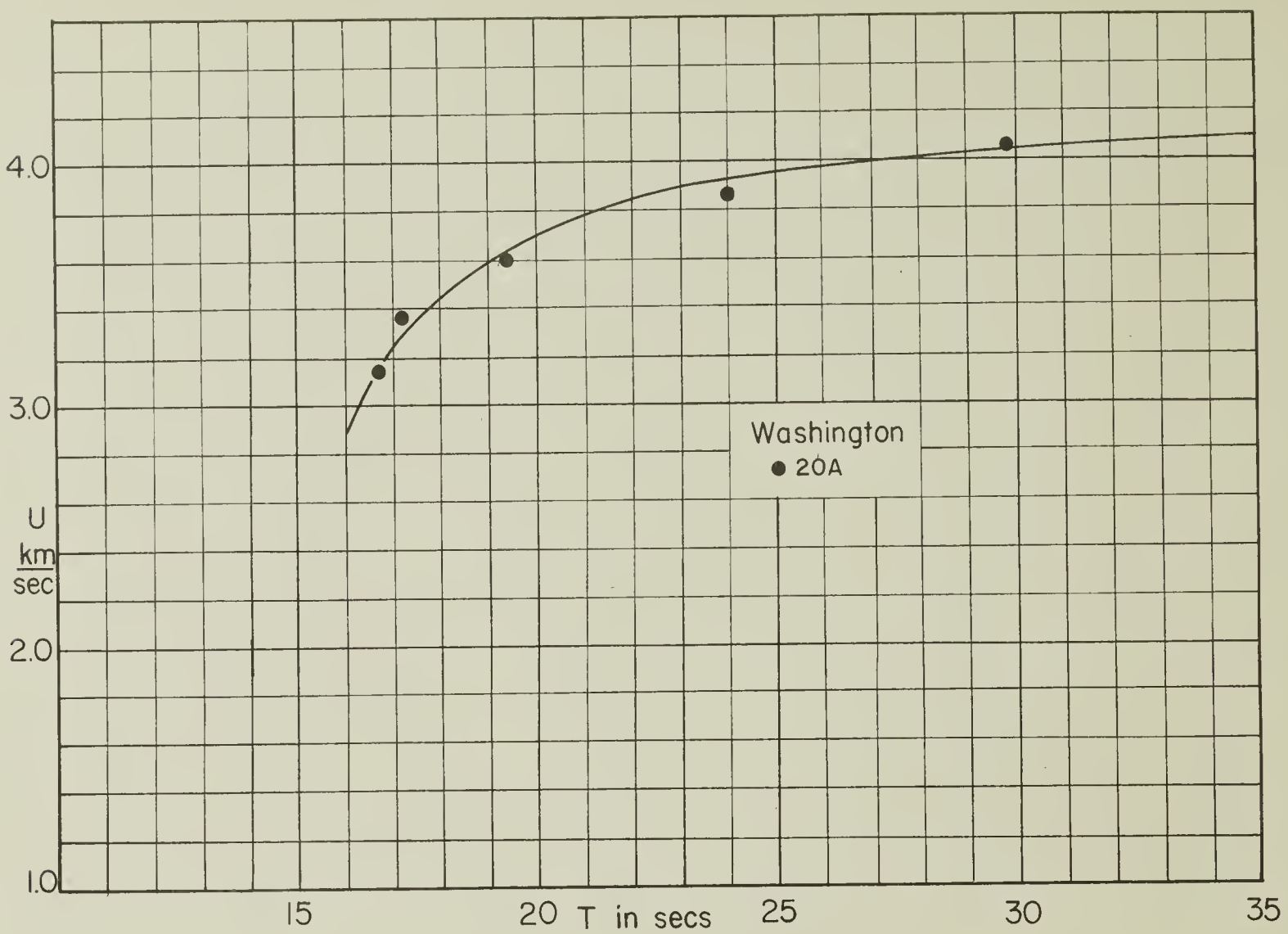

Figure 14. Rayleigh Wave Dispersion, Washington (Table 1)

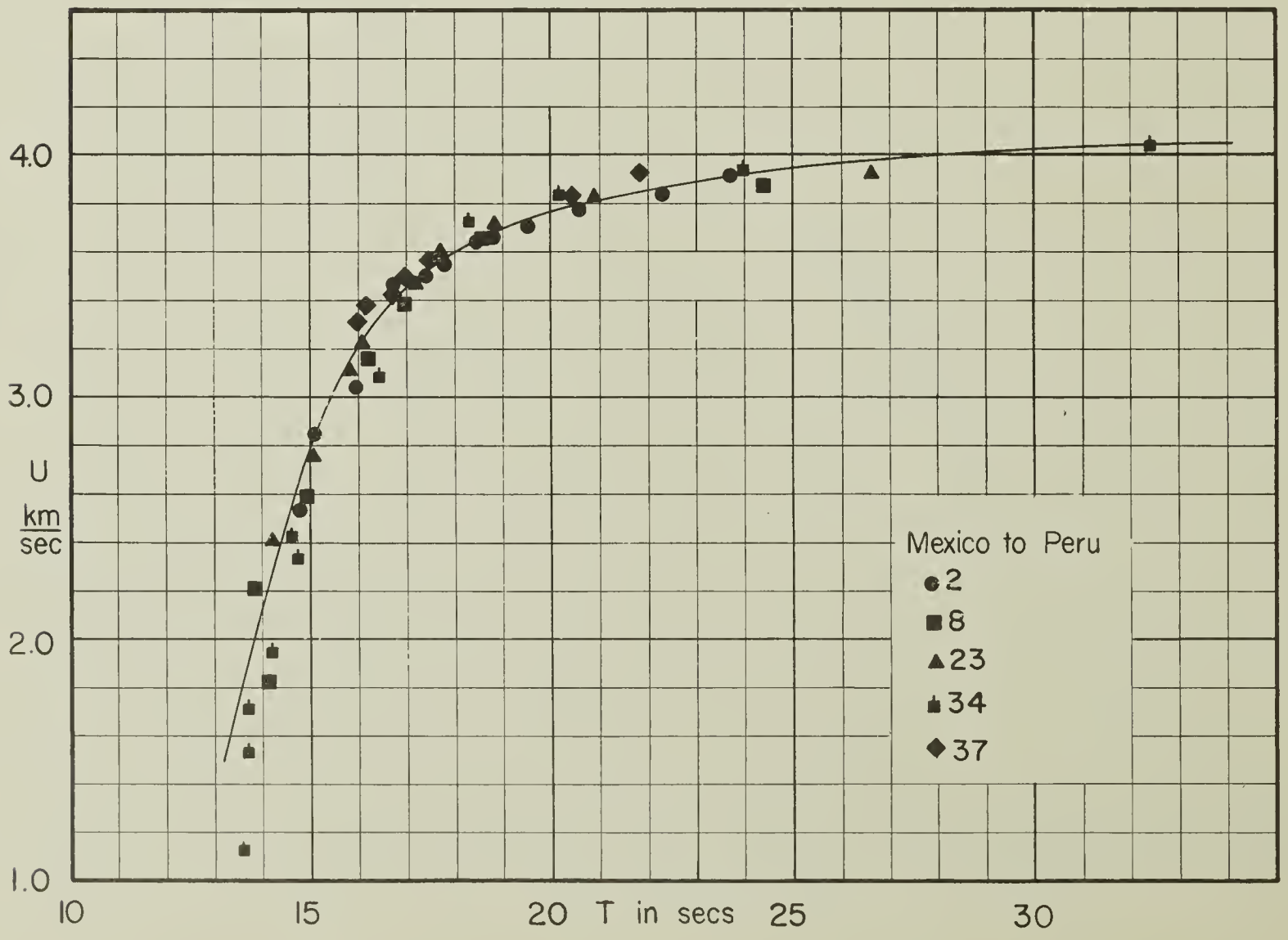

Figure 15. Rayleigh Wave Dispersion, Mexico to Peru (Table 1)

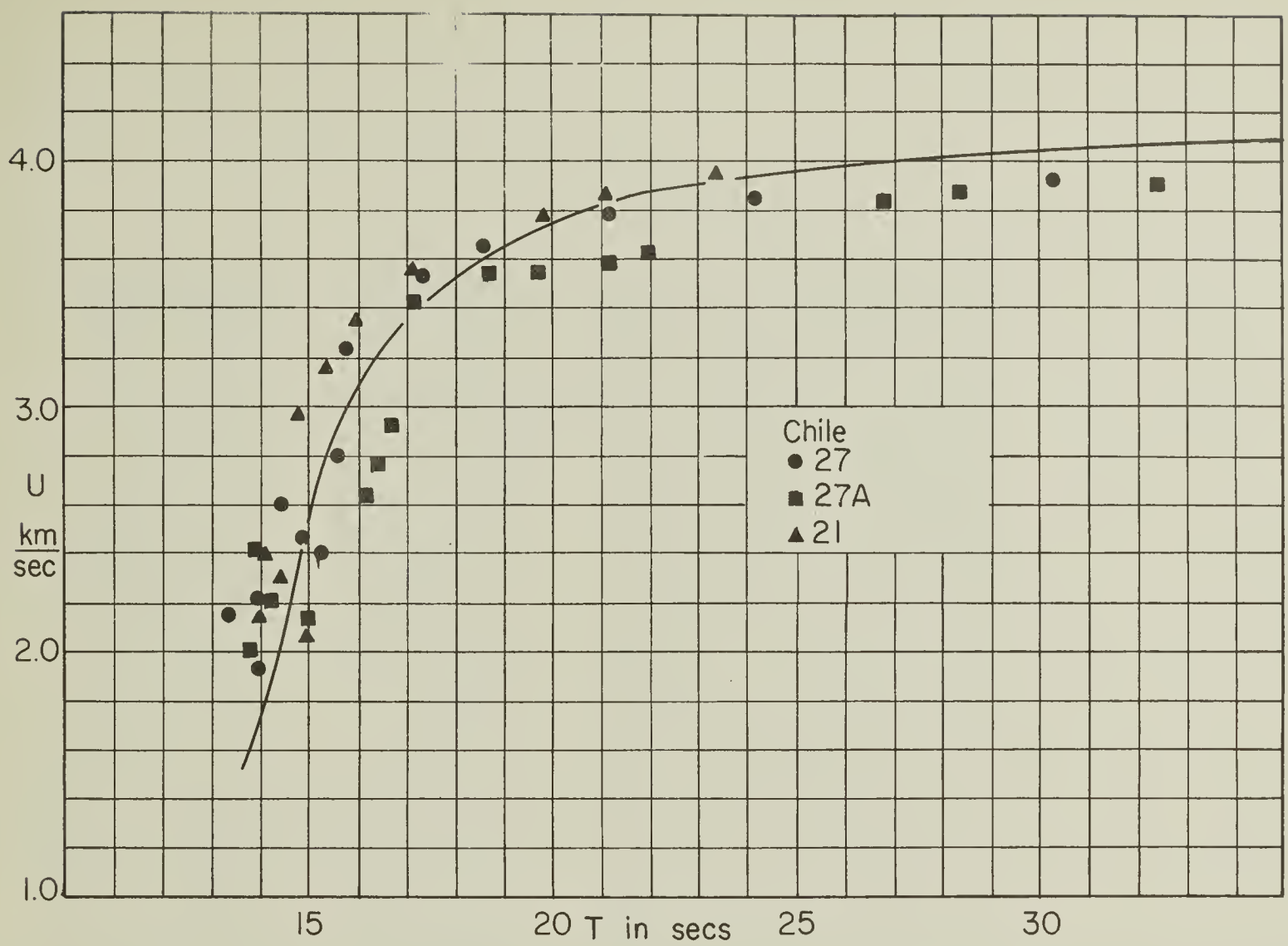

Figure 16. Rayleigh Wave Dispersion, Chile (Table 1)

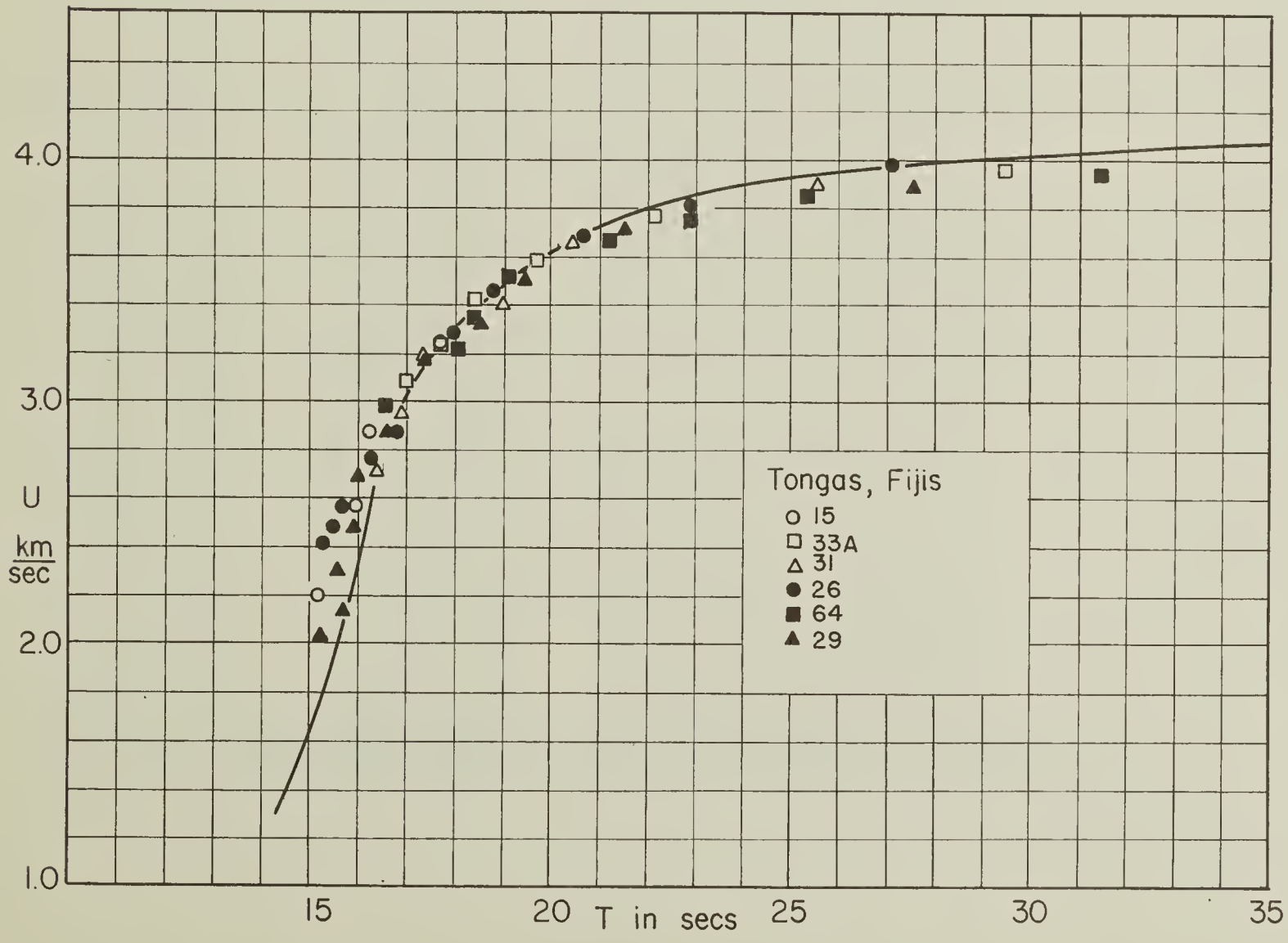

Figure 17. Rayleigh Wave Dispersion, Tongas, Fijis (Table 1)

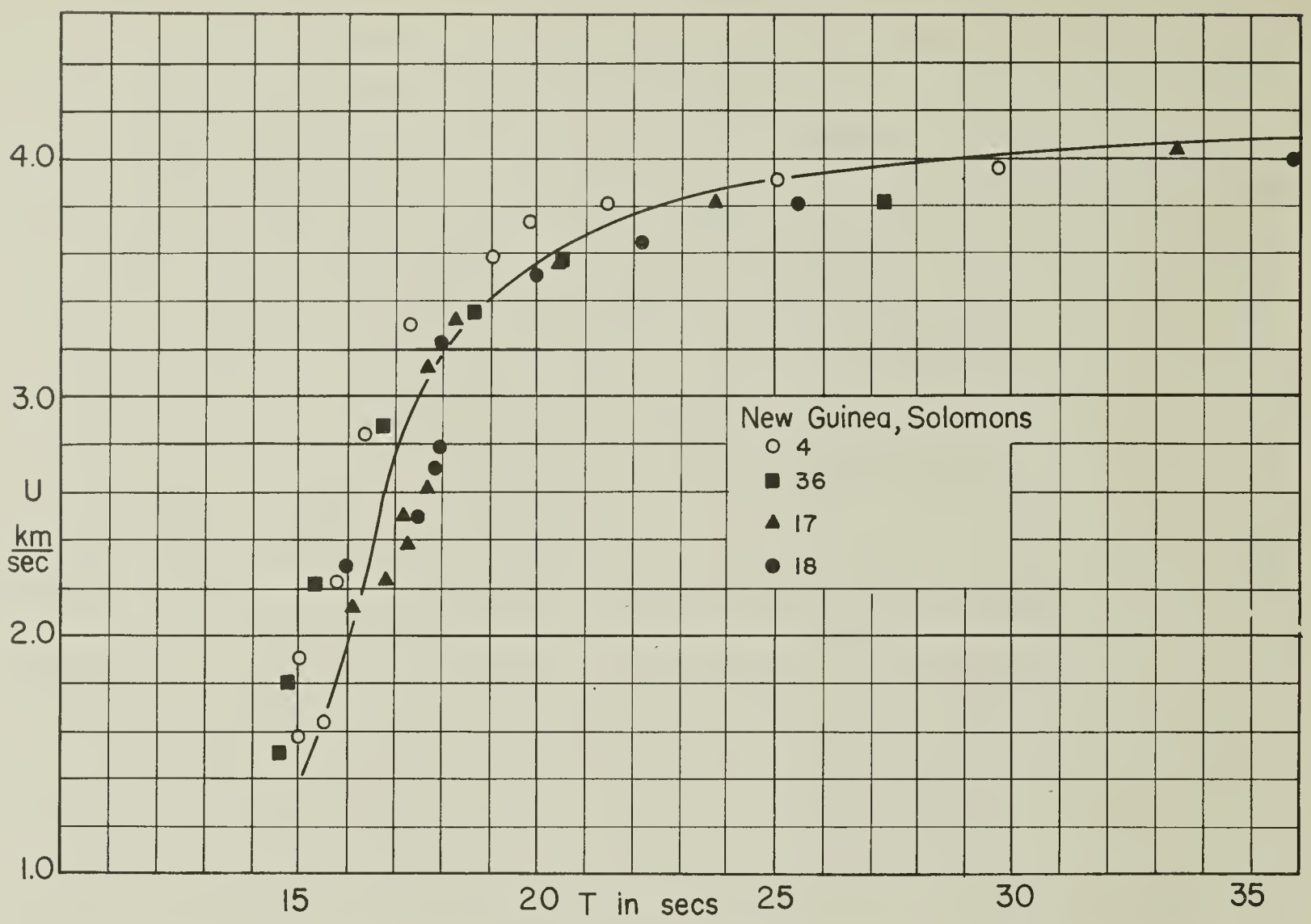

Figure 18. Rayleigh Wave Dispersion, New Guinea, Solomons (Table 1)

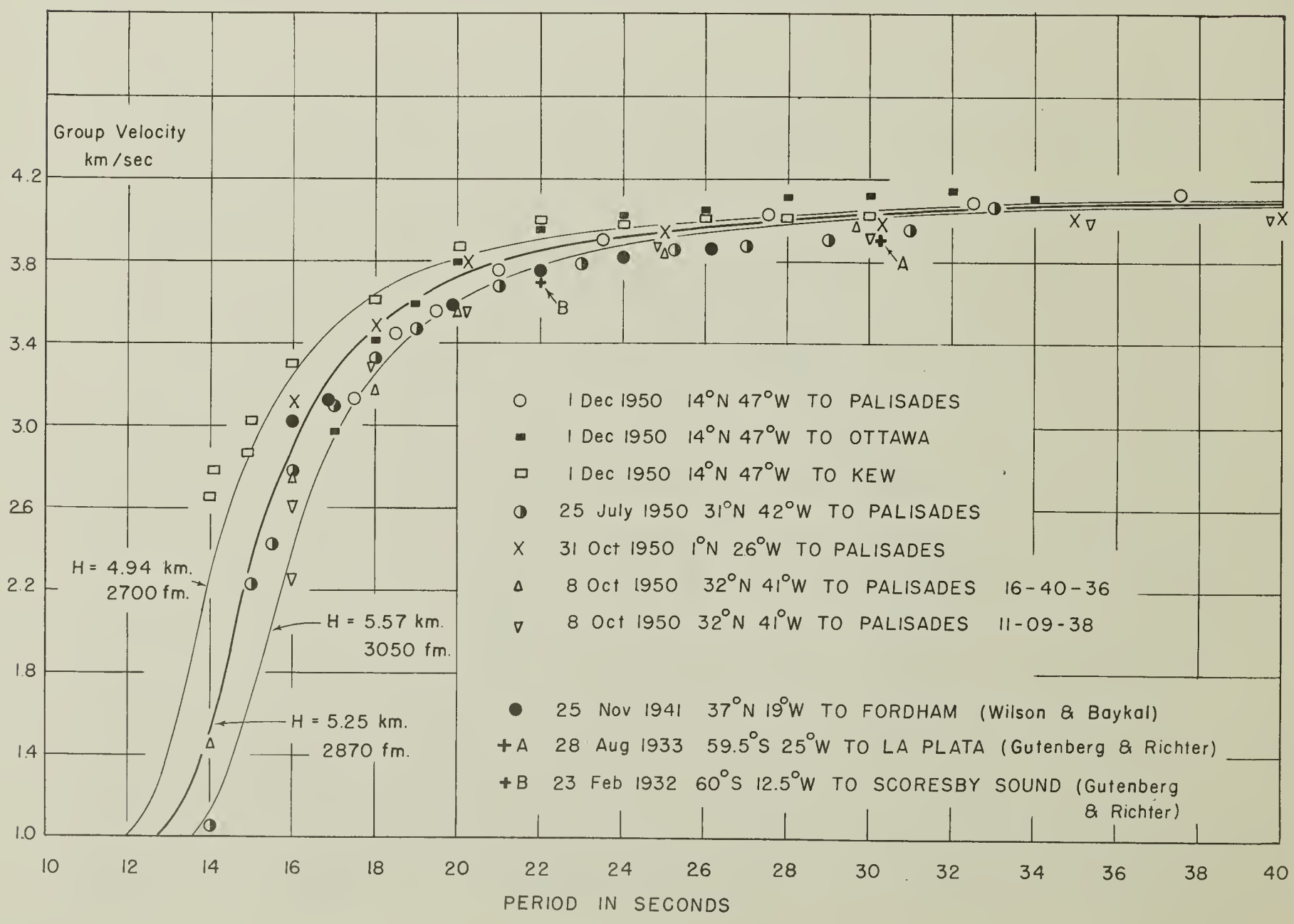

Figure 19. Rayleigh Wave Dispersion, Atlantic (Table 3)

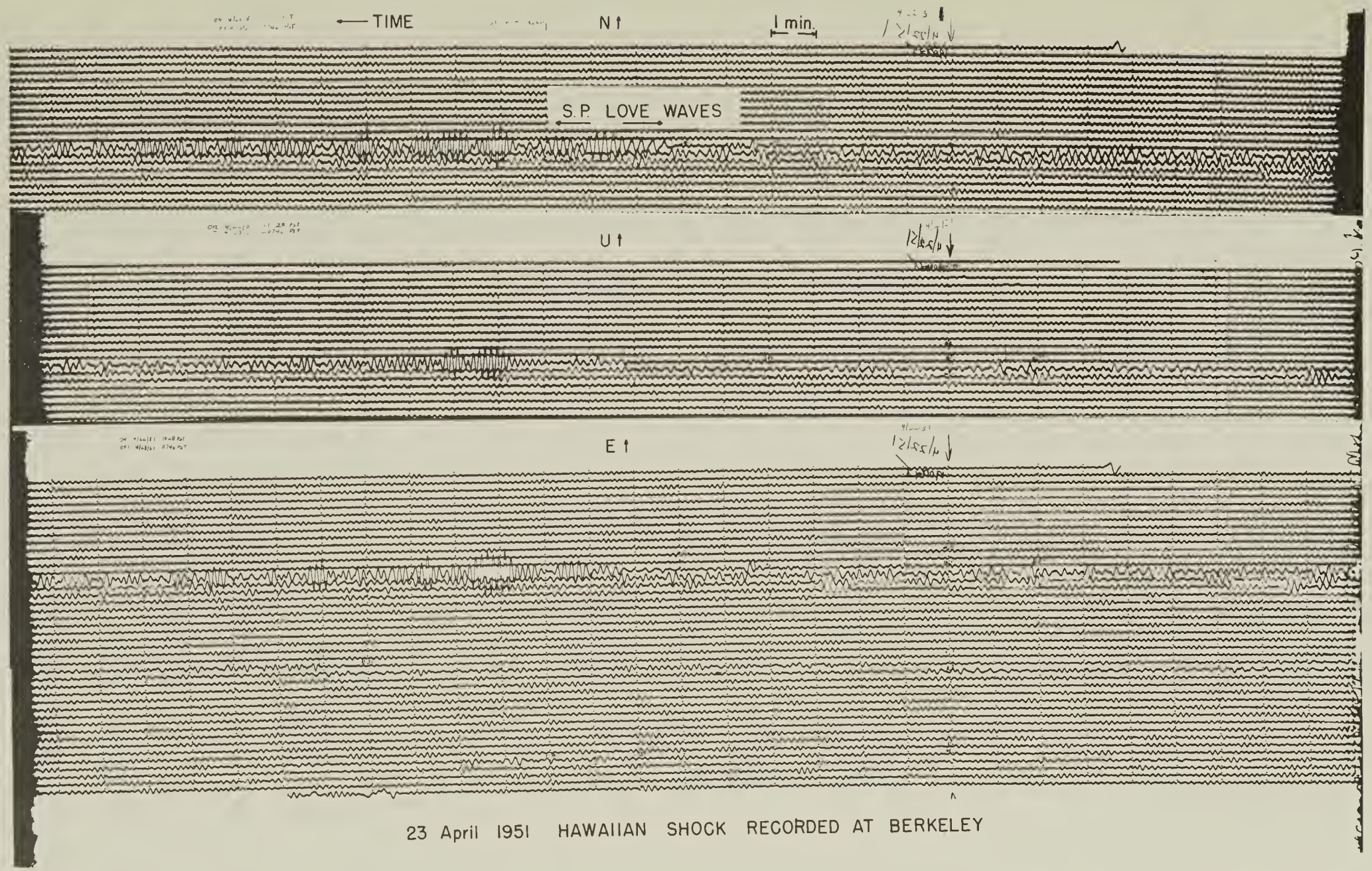

Figure 20. Short Period Surface Waves, Berkeley Records (Table 2)

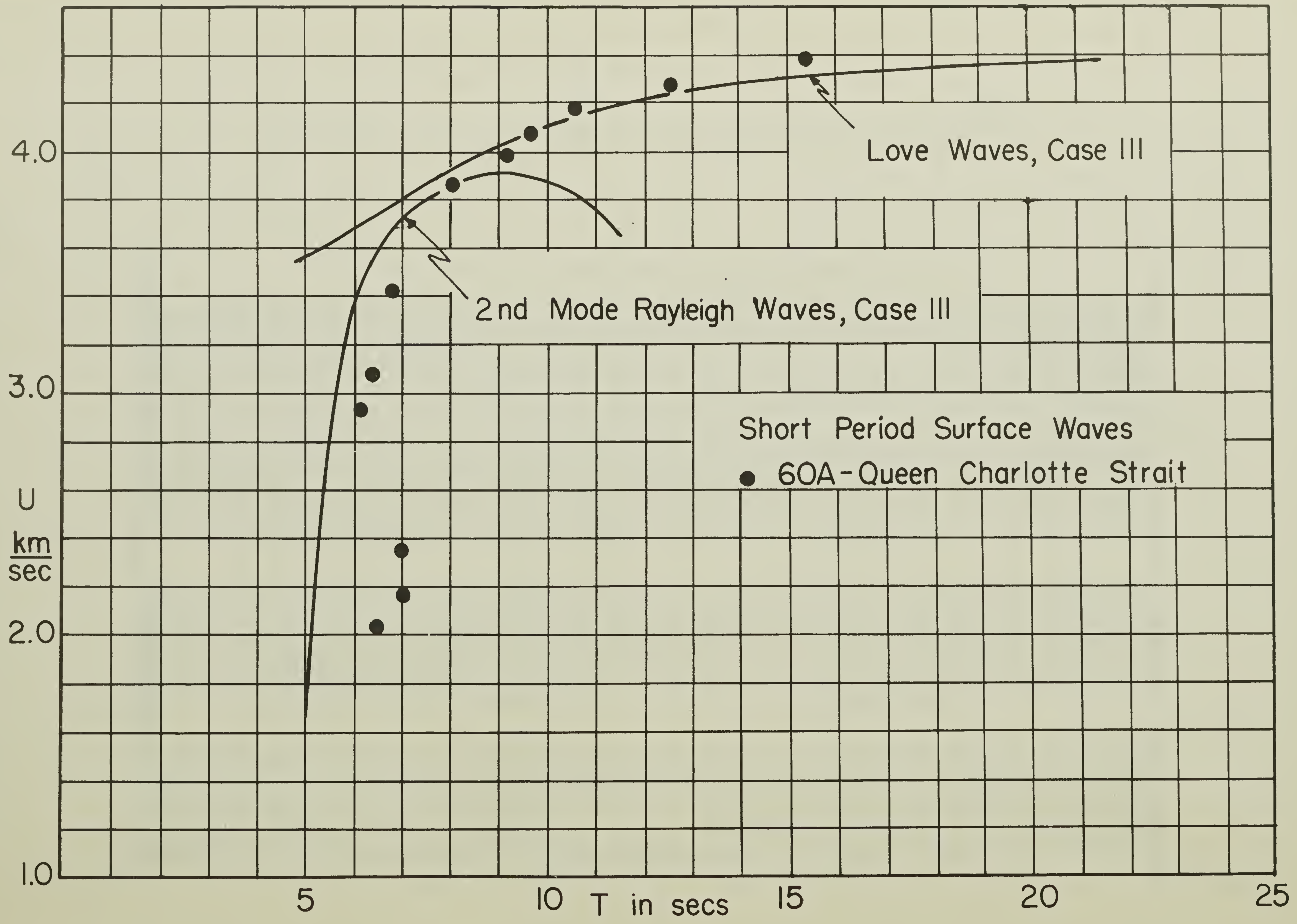

Figure 21. Short Period Surface Wave Dispersion (Table 1)

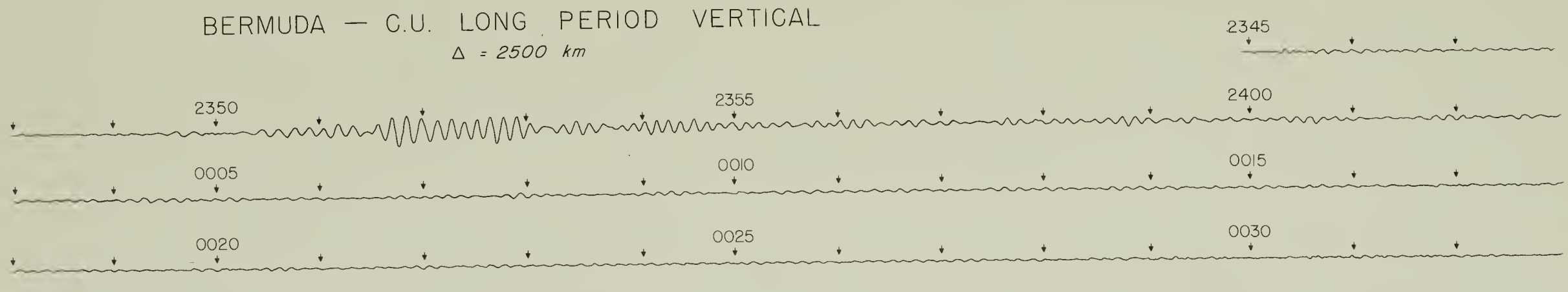

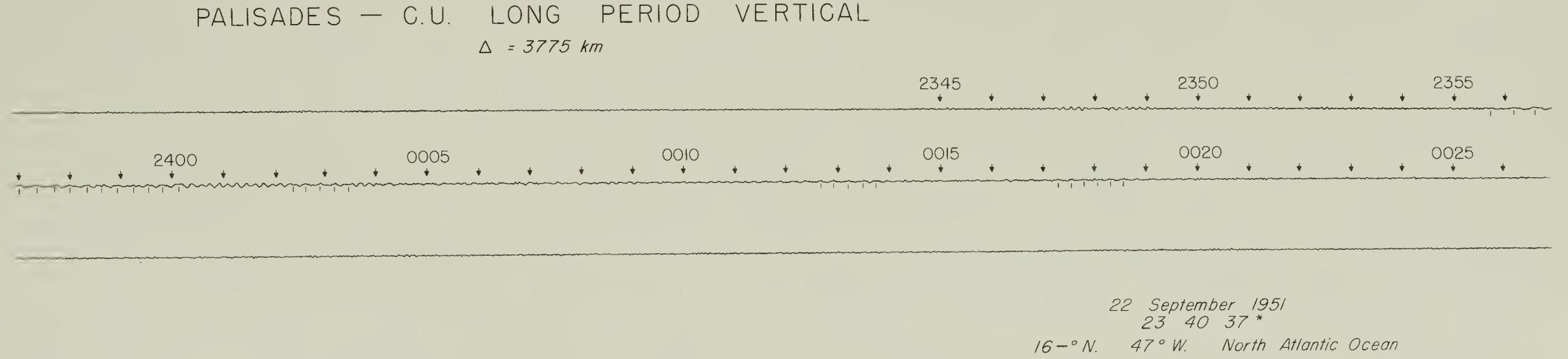

Figure 22. Short Period Surface Waves, Palisades and Bermuda Records (Table 3)